

CHAPTER 1

Survey of the Properties of Water

Personal Introduction

My interest in the properties of water started while I was working on my PhD thesis in the early 1960s. My thesis focused on the outstanding properties of aqueous solutions of inert gases. It was clear then that the understanding of the properties of aqueous solutions hinged upon the understanding of the properties of liquid water.

I started to work on the theory of water only in my second year as a post-doctoral fellow at Bell-Labs with Frank Stillinger. For almost two years (1967–1968), I tried to construct a water-water pair potential. Most of the time was spent in determining the parameters of the potential function so that it would fit the experimental molecular properties such as dipole moment, second virial coefficient, and compressibility of ice (see Chapter 2).

I did not do any experimental work on pure water. All of the data reported in this chapter were either taken directly from the literature or derived from these data. Two relatively less known quantities are reported in Secs. 1.5 and 1.6. These quantities convey important local information derived from experimental data. The data that I used in my earlier book, published in 1974, were taken mainly from the Dorsey (1940) compilation. At that time, the book of Eisenberg and Kauzmann (1969) was also published. It summarized both the experimental and theoretical works on water. Fletcher's book (1970) summarized what

was known on the properties of ice. Most of the experimental data reported in this chapter were taken from NIST compilations.¹ The molecular interpretation of these properties will be discussed in Chapter 2.

1.1. Introduction and Some Historical Notes

In this chapter, we shall survey some of the most outstanding properties of liquid water. We shall begin with some historical notes on the earlier theories of water and aqueous solutions, and end this chapter with some notes on the relevance of the outstanding properties of water to life. To understand *liquid* water, it is necessary to be familiar with the properties of water in the gaseous phase, as well as in the solid phase. We shall briefly review these systems in Secs. 1.2 and 1.3. The outstanding properties of liquid water will be described in Secs. 1.4 through 1.6.

In anticipating the theoretical interpretation in Chapter 2, we can roughly divide the properties of water into two groups. The first includes properties such as the large heat capacity, the low solubility of inert solute, and hydrophobic interactions. At the molecular level, these were traditionally interpreted in terms of hydrogen bonds (*HBs*). This is basically true. However, the *HB*, *per se*, is not essential to the understanding of these properties. What is essential is the *strength* of the water-water interaction. Other liquids, with strong intermolecular interactions (whether by *HBs* or otherwise) will show similar behavior. As we shall see in Chapter 2, strong interactions or *HBs* by themselves do not reproduce any of the outstanding properties of water. Here, we emphasize that the strong interactions between water molecules are more fundamental than *HBs*.

¹Lemmon *et al.* (2007).

The second group consists of properties that are seemingly, as far as it is known, unique to liquid water.² Examples are the negative temperature dependence of the volume, the large negative entropy of solvation of inert solute, etc. These properties were traditionally interpreted at a molecular level in terms of the *tetrahedral structure* of ice — which also persists in liquid water. As we shall see throughout this book, the tetrahedral structure, though an important feature of water, is not essential to the understanding of water. What is essential is the unique correlation between low local density, and strong binding energy, as illustrated in the cover design and further elaborated on in Chapter 2.

The outstanding properties of liquid water were recognized long ago. A compilation of the properties of liquid water was first published in 1940 by Dorsey. Some of the outstanding properties of water were also discussed by Pauling (1940, 1960), Kavanau (1964), and Samoilov (1957) (the latter two are more concerned with the properties of aqueous solutions). The relevance of water to biology was discussed by Henderson (1913), Edsall and Wyman (1958), and Franks (2000). The modern era in the research on water started in the late 1960s with the publication of the Eisenberg and Kauzmann book in 1969. This was followed by a book on the molecular properties of liquid water (Ben-Naim, 1974). During the 1970s, a series of books were published by Franks (1973–1982) including chapters on specific topics written by specialized authors. A more recent book by Robinson *et al.* (1996) summarizes both the experimental and the theoretical advances in the field. An interesting, more descriptive book was also published by Ball (1999).

²For some exceptions, see Angell *et al.* (2000).

In this chapter, we shall survey some of the outstanding properties of pure water in the gaseous, liquid, and solid phases. We shall discuss only equilibrium thermodynamic quantities. Properties of aqueous solutions are deferred to Chapters 3 and 4.

1.2. Properties of Water in the Gaseous Phase

1.2.1. *The single water molecule*

In order to understand the properties of liquid water and its role in biological systems, one must be familiar with the basic properties of a single water molecule.

The notation H_2O for the water molecule shows the *composition* but not the geometry of the molecule. The structure of a single water molecule has long been established such that the nuclei of the oxygen atom and the two hydrogen atoms form an isosceles triangle (Fig. 1.1). The equilibrium³ O-H bond length is 0.957 \AA ,⁴ and the H-O-H angle is equal to 104.52° .⁵ Note that this angle is smaller than the tetrahedral angle of 109.46° . The latter is an important quantity that we shall frequently encounter in this book (see also Appendix A).

This particular geometry has been established by a number of experiments utilizing a variety of methods as well as by theoretical calculations.⁶ For most of our studies of the properties of liquid water, we can assume that a water molecule has a *rigid* geometry with a fixed bond length and a fixed bond angle.

³Note that the two atoms O and H forming the bond O-H are not at a fixed distance. There are incessant vibrations that change the bond length. Therefore, we refer here to the equilibrium or the average bond length.

⁴One Ångström (Å) equals 10^{-8} cm.

⁵This is again an equilibrium or an average angle.

⁶For example, the heat capacity of water corresponds to three translational and three rotational degrees of freedom. Also from the dielectric constant of water vapor, one can determine the dipole moment of a single water molecule. These facts, as well as others, indicate that water is not a linear molecule.

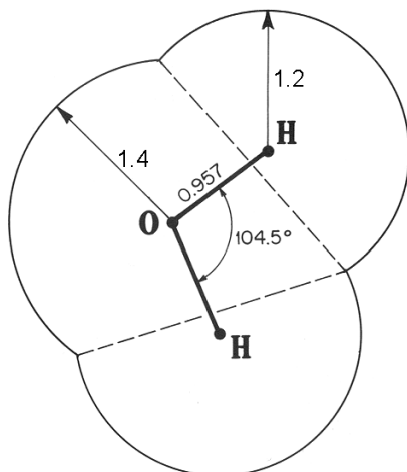


Fig. 1.1 The geometry of a single water molecule. The van der Waals radii of the hydrogen and oxygen atoms are indicated (in Å).

This simplified model is not sufficient for studying properties that are affected by the vibrations of a single water molecule, or by the dissociation of the molecule into charged ions H^+ and OH^- .

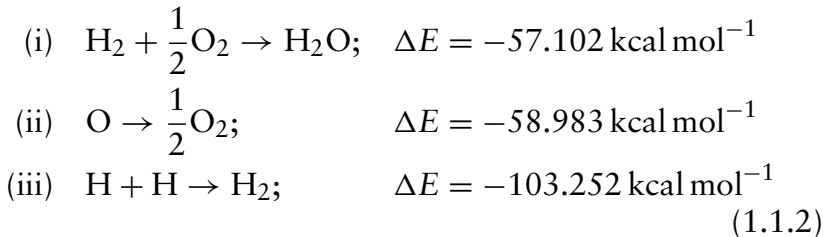
In this book we shall not discuss dissociation of a water molecule into either the ions H^+ or OH^- or to the neutral components hydrogen or oxygen. However, it is important to have an idea of the order of magnitude of the energies involved in the formation of a water molecule.

The energy of formation of a molecule H_2O is defined for the process



where H and O are the hydrogen and the oxygen atoms at the electronic ground state, and the water molecule is in the electronic, vibrational, rotational, and translational ground states, i.e. we carry out the hypothetical process (1.1.1) at absolute zero temperature. The energy associated with reaction (1.1.1) is

calculated from the energies of the following processes:



Thus, we have

$$\text{(i)} + \text{(ii)} + \text{(iii)} = \text{(1.1.1)}; \quad \Delta E = -219.337 \text{ kcal mol}^{-1}
 \tag{1.1.3}$$

Note that the *electronic binding energy* is different from the energy of formation of the water molecule, the difference between the two being the zero point energy given in Table 1.1.

The motion of a water molecule may be described in terms of two components: (i) the motion of the center of mass of the entire molecule (this includes both translation and rotations) and (ii) the relative motions of the atoms within the molecule. The latter may be described in terms of three fundamental (“normal”) modes of vibration (see Fig. 1.2).

In Table 1.1, the frequencies ν_i ($i = 1, 2, 3$) correspond to the transition from the ground state (of all the vibrational modes) to the first vibrational level of the i th mode of vibration.⁷ The zero point energy of H₂O and of D₂O are also given in Table 1.1. For more details, see Eisenberg and Kauzmann (1969).

In Table 1.2 we present some data on the molecular properties of a single water molecule. All the values in the table pertain to the hypothetical “equilibrium state” of the molecule, i.e. a molecule that does not vibrate or rotate. Note also that the bond lengths and bond angles of H₂O and D₂O are nearly the same.

⁷It is easy to show that at room temperature less than 0.1% of the molecules are in any one of the excited vibrational states.

Table 1.1. The Vibrational Frequencies and Zero Point Energies of H₂O and D₂O^a

	H ₂ O	D ₂ O
ν_1 , symmetric stretching	3656.65	2671.46
ν_2 , asymmetric stretching	3755.79	2788.05
ν_3 , bending vibration	1594.59	1178.33
Zero point energy	4634.32	3388.67
	(13.2 kcal mol ⁻¹)	(9.8 kcal mol ⁻¹)

^aFrom Eisenberg and Kauzmann (1969), based on data from Benedict *et al.* (1956) and Herzberg (1950). Values of ν_1 , ν_2 , and ν_3 are in cm⁻¹. 1 cm⁻¹ corresponds to 2.859 cal mol⁻¹.

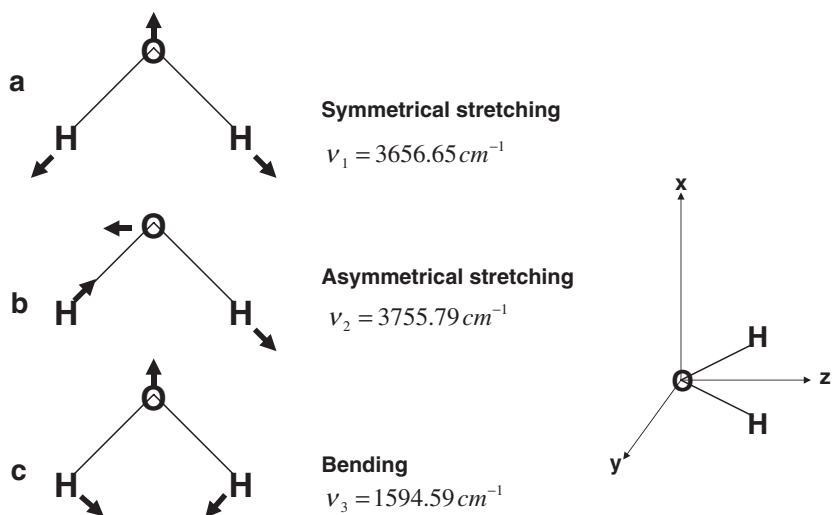


Fig. 1.2 The normal modes of vibration of a single water molecule. The first two vibrations (a) and (b) are referred to as the stretching vibrations with the corresponding frequencies ν_1 and ν_2 . The third (c) is referred to as the bending vibration, with frequency ν_3 .

In studying liquid water and aqueous solutions, most of the time we will be able to ignore both the internal motions (vibrations) of the atoms within molecules, and the dissociation of water molecules into their ionic components. This latter dissociation

Table 1.2. Molecular Properties of H₂O and D₂O^a

	H ₂ O	D ₂ O
Bond length × 10 ⁸ cm	0.9572	0.9575
Bond angle	104.523°	104.474°
Moment of inertia		
$I_x \times 10^{40}$ g cm ²	2.9376	5.6698
$I_y \times 10^{40}$ g cm ²	1.9187	3.8340
$I_z \times 10^{40}$ g cm ²	1.0220	1.8384

^aFrom Eisenberg and Kauzmann (1969) based on measurements by Benedict *et al.* (1956), all entries in this table refer to the equilibrium values. The *x*-axis passes through the center of mass of the molecule and is perpendicular to the plane of the molecule. The *z*-axis is a bisection of the bond angle, and the *y*-axis is perpendicular to *x* and *z* (Fig. 1.2).

phenomenon is important when we are interested in the acidity of aqueous solutions. Thus, our initial assumption is that a single water molecule has a fixed and rigid geometry. Since an oxygen atom is 16 times heavier than a hydrogen atom, the center of mass of the oxygen atom is approximately the same as the center of mass of the entire water molecule.

The geometry of a water molecule, as depicted in Fig. 1.1, takes into account only the *nuclei* of the three atoms. Of course, there are also electrons moving about these nuclei. This “cloud” of electrons gives rise to the notion of the “volume” of the water molecule. This molecular volume is not a well-defined concept; it is not like the concept of the volume of a (macroscopic) geometrical solid such as a sphere or a cube. Since the electrons are “spread” about the three nuclei, there exists no well-defined boundary to the water molecule. Nevertheless, we do assign an effective radius (hence volume) to each atom, referred to as the van der Waals radius of an atom, which is 1.4 Å for an oxygen atom and 1.2 Å for a hydrogen atom. With these van der Waals

radii, we can view the water molecule as though it has an *effective* solid structure. It is sometimes convenient to view a water molecule as a sphere of radius 1.41 Å. (This radius is about half of the average distance between two closest water molecules as manifested by the first peak of the radial distribution function of water discussed in Sec. 1.4.5).

One more important property of the single water molecule that we need to define is the electric dipole moment. The nuclei and the electrons in each atom are charged particles — the positive nucleus and negative electrons. Since the total number of positive charges equals the total number of negative charges, the molecule as a whole is electrically neutral. However, the distribution of charges is not spherically symmetric; therefore, the water molecule as a whole is polar. The polarity of the molecule is a measure of the asymmetry in the distribution of the charged particles. This may be presented by a sum of electric multipoles,⁸ the first and the most important of which is the electric dipole moment.

The simplest example of a charge distribution would be two point charges of equal magnitude (e.g. $\pm q$), one positive and the other negative, separated by a distance d (Fig. 1.3). The strength of the dipole moment is $\mu = q \cdot d$, i.e. the charge multiplied by

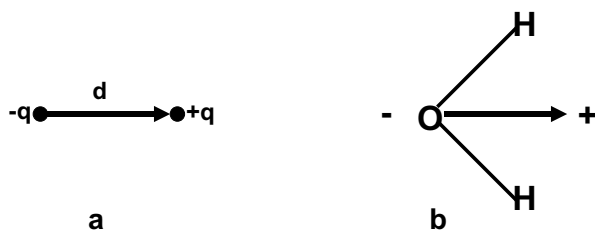


Fig. 1.3 (a) A dipole moment of two point charges at a distance d . (b) The direction of the dipole moment vector of a water molecule.

⁸For more details, see Bottcher (1952) and Jackson (1952).

the distance separating the two points. In a water molecule, the distribution charges are more complicated than this. One can assign dipole, quadrupole, octupole, etc. moments. The strength of the dipole moment denoted μ of a water molecule is 1.84×10^{-18} e.s.u. cm (electrostatic unit \times centimeters) or 1.84 Debye.⁹ The dipole moment is a vector, the direction of which is usually designated from the negative to the positive charge.¹⁰ It has been established that the overall charge distribution of a water molecule produces a dipole moment that originates at the center of the oxygen atom and is directed along a line bisecting the angle H-O-H (see Fig. 1.3b). Values of higher multipoles are also known. For details, see Eisenberg and Kauzmann (1969) and Fletcher (1970).

1.2.2. *Interaction between two water molecules*

In the previous section, we presented the basic properties of a single water molecule. We now discuss the various ways two water molecules can interact. As we shall see in the following sections, knowledge of these interactions is essential to our understanding of the properties of liquid water and aqueous solutions.

What is a pair interaction? In the context of this book, the term “interaction” is an abbreviation for *interaction energy*.¹¹ In order to define the interaction energy between any two particles, we consider first two spherical atoms, e.g. two argon atoms. The interaction energy between two atoms at a distance R is defined as the difference in *energy* when we move the two atoms

⁹1 Debye = 10^{-18} e.s.u. cm.

¹⁰In chemistry, the dipole vector is defined from the positive to the negative charge.

¹¹In the literature, the term “interaction” is also used for what is referred to as the potential of mean force. This is discussed in Chapter 4.

from an infinite separation to a distance R . We denote this interaction energy by

$$U(R) = E(R) - E(\infty) \quad (1.2.1)$$

Note that we use here a “thought experiment” to define the interaction energy. We start with two atoms at rest (i.e. no kinetic energy) at infinite separation (∞), bring them to a distance R , and calculate the change of energy or the work done in this process. Clearly, such a process cannot be carried out in the laboratory. However, we can calculate the general form of the function $U(R)$ either by pure theoretical means, or from some experimental measurement that we can perform¹² (for instance, measuring deviations from ideal gas behavior, viscosity of gases, etc). From these calculations we get the general form of the function $U(R)$, which we call the pair potential or the pair-interaction energy. Figure 1.4 shows the qualitative form of this function for neon, argon, krypton, and xenon.

The curves for this illustration were obtained from the Lennard–Jones (LJ) function

$$U(R) = 4\varepsilon \left[\left(\frac{\sigma}{R} \right)^{12} - \left(\frac{\sigma}{R} \right)^6 \right] \quad (1.2.2)$$

with parameters given in Table 1.3.

The region of positive values of $U(R)$ is referred to as the repulsive part of the interaction. To reach this region, work must be done in order to push the two particles to a distance smaller than the effective diameter of the spherical atom, σ .¹³ On the other hand, energy is released when the two particles are brought to a distance greater than σ . As can be seen in Fig. 1.4,

¹²See, for example, Hirschfelder *et al.* (1954).

¹³In this preliminary discussion, we ignore the difference between σ , which is the location where $U(R = \sigma) = 0$, and the minimum of the function $U(R)$, which is at $\sqrt[6]{2}\sigma$.

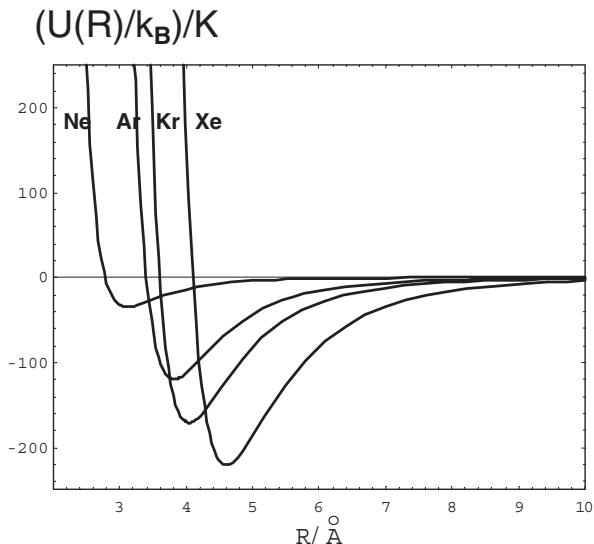


Fig. 1.4 The pair potential for neon, argon, krypton, and xenon.

Table 1.3. Values of σ and of ϵ/k_B for the Lennard–Jones Function Fitted to Obtain the Second Virial Coefficient of Inert Gases^a

Gas	σ (Å)	ϵ/k_B (K)
Ne	2.78	34.9
Ar	3.40	119.8
Kr	3.60	171.0
Xe	4.10	221.0

^aFrom Hirschfelder *et al.* (1954).

the potential rises steeply for $R < \sigma$. We usually refer to σ as the van der Waals diameter of the particles. It is a “diameter” in the sense that two particles cannot penetrate into each other to a distance smaller than σ . Note also that a negative slope in the pair potential corresponds to a repulsive *force*, a positive slope corresponds to an attractive force between the two particles.

All we have said thus far is valid for spherical particles such as argon atoms for which the interaction energy is a function only of the distance R . Next, we describe a few simple interaction potentials. The interaction energy between two point charges, q_1 and q_2 , at a distance R , is given by Coulomb's law, i.e.¹⁴

$$U(R) = \frac{q_1 q_2}{R} \quad (1.2.3)$$

By extending Eq. (1.2.3), we can write the interaction energy between a point charge q_1 and a dipole (Fig. 1.5). It is clear that the interaction energy here depends on the orientation of the dipole moment. If we view the dipole as a combination of two-point charges (of charges $+q$ and $-q$ at distance d apart), then we can write the interaction energy between a charge q_1 and the dipole as simply the sum of two Coulombic interactions, namely (Fig. 1.5)

$$U(R_1, R_2) = \frac{q_1 q}{R_1} - \frac{q_1 q}{R_2} \quad (1.2.4)$$

Coulomb's law can be extended further for a *pair* of dipoles (see Fig. 1.6). Again, we can sum up all the Coulombic interactions between the four point charges (excluding here the two interactions between charges belonging to the same dipole). Thus, we write (Fig. 1.6)

$$U(R_1, R_2, R_3, R_4) = \frac{q^2}{R_1} + \frac{q^2}{R_2} - \frac{q^2}{R_3} - \frac{q^2}{R_4} \quad (1.2.5)$$

Note that we have assumed here that all point charges have the same magnitude q .

In most applications, we do not need Eq. (1.2.5) for the dipole-dipole interaction. Instead, we need only the interaction between two dipoles when the distances R_i ($i = 1, 2, 3, 4$) are all

¹⁴Here, we show only the functional form of Coulomb's law; in order to fix the units, we would need to add a constant to the right-hand side of the equation.

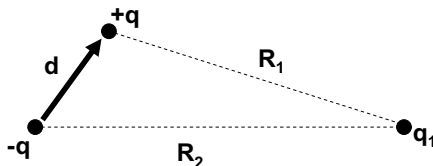


Fig. 1.5 The interaction between a point charge (q_1) and a dipole.

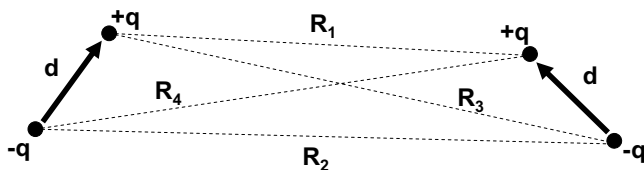


Fig. 1.6 The interaction between two dipoles is a result of the interactions between the four pairs of point charges.

very large compared to the distance d — in which case we say that we have two point-dipoles¹⁵ of strength $\mu = qd$, and the interaction between them is given by

$$U(R) = \alpha \frac{\mu^2}{R^3} \quad (1.2.6)$$

Here, R is the distance between the two point-dipoles, and α depends on (i) the orientation angles of the two dipoles, relative to the line connecting the two point-dipoles, and (ii) the dihedral angle of rotation between the dipoles (Fig. 1.7).

The most important aspect of the dipole-dipole interaction in Eq. (1.2.6) is that the interaction energy changes with distance as R^{-3} , whereas the Coulombic interaction between two charges changes with distance as R^{-1} . In general, the interaction energy

¹⁵A point-dipole is defined as the product of q and d when $q \rightarrow \infty$ and $d \rightarrow 0$, but the product $q \times d$ remains constant.

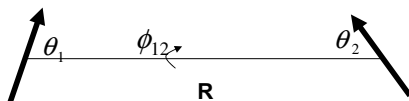


Fig. 1.7 The interaction energy between two dipoles depends on the distance R and the three angles θ_1 , θ_2 , and ϕ_{12} [Eq. (1.2.10)].

between two dipoles depends on four parameters: one distance and three angles.

The interaction energy between two water molecules is more complicated than the dipole-dipole interaction. Here, we shall describe some of the general features of this function.

As we indicated above, the pair potential between two water molecules is a complicated function of the distance R and the five orientation angles. The exact analytical form of this pair potential is not known.¹⁶ Earlier models of water were proposed by Bernal and Fowler (1933), Verwey (1941), Bjerrum (1951), Stockmyer (1941), Rowlinson (1951), and others. All these failed to reproduce the characteristic radial distribution of water (see Sec. 1.4.5). What one usually uses in the theory of water is not the true pair potential¹⁷ but an *effective* pair potential consisting of essentially three parts, which we write as

$$U(\mathbf{X}_1, \mathbf{X}_2) = U_{LJ}(R) + U_{DD} + U_{HB} \quad (1.2.7)$$

The first part, $U_{LJ}(R)$ is a Lennard–Jones (*LJ*) potential that has the general form as in Eq. (1.2.2), where ε and σ are parameters that approximately equal the parameters used to describe the pair potential between two neon atoms. $\varepsilon = 5.01 \times 10^{-15} \text{ erg} = 7.21 \times 10^{-3} \text{ kcal mol}^{-1}$, $\sigma = 2.82 \text{ \AA} = 2.82 \times 10^{-8} \text{ cm}$. Note that for $R = \sigma$, the pair potential is

¹⁶It is not clear that an exact analytical form of a pair potential exists.

¹⁷As we shall discuss in Chapter 2, the “true” pair potential in itself is not essential for understanding the behavior of water.

zero (see Fig. 1.4). On the other hand, the minimum of the *LJ* potential is obtained at $R_{\min} = \sqrt[6]{2}\sigma$, where the value of the potential is

$$U(R_{\min}) = -\varepsilon \quad (1.2.8)$$

Hence, σ measures the “size” of the particles, and ε the strength of the interaction energy between the particles.

The *LJ* part of the potential is used mainly to account for the repulsive interaction when the two molecules come to a very short distance $R \leq \sigma$. Sometimes, instead of an *LJ* potential of the form (1.2.2), one uses a hard-sphere (*HS*) potential, defined by (Fig. 1.8)

$$U_{HS}(R) = \begin{cases} \infty & \text{for } R \leq \sigma \\ 0 & \text{for } R > \sigma \end{cases} \quad (1.2.9)$$

The second part, U_{DD} , is the dipole-dipole interaction. For two point-dipoles μ_1 and μ_2 at locations \mathbf{R}_1 and \mathbf{R}_2 , the

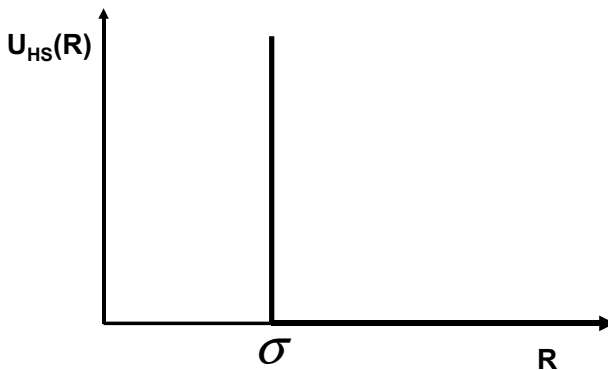


Fig. 1.8 The interaction potential function for a pair of hard spheres of diameter σ [Eq. (1.2.9)].

dipole-dipole interaction is

$$\begin{aligned}
 U_{DD}(\mathbf{R}_1, \boldsymbol{\Omega}_1, \mathbf{R}_2, \boldsymbol{\Omega}_2) & \\
 &= \frac{(\boldsymbol{\mu}_1 \cdot \boldsymbol{\mu}_2) - 3(\boldsymbol{\mu}_1 \cdot \mathbf{u}_{12})(\boldsymbol{\mu}_2 \cdot \mathbf{u}_{12})}{|\mathbf{R}_1 - \mathbf{R}_2|^3} \\
 &= \frac{-\mu^2}{R^3} (2 \cos \theta_1 \cos \theta_2 - \sin \theta_1 \sin \theta_2 \cos \phi_{12}) \quad (1.2.10)
 \end{aligned}$$

where $\mu_i = |\boldsymbol{\mu}_i|$ is the dipole moment of the particle i and \mathbf{u}_{12} is a unit vector along $\mathbf{R}_1 - \mathbf{R}_2$ and $R = |\mathbf{R}_1 - \mathbf{R}_2|$, is the distance between the two dipoles. The brackets on the right-hand side of (1.2.10) are the scalar products between the two vectors. The angles θ_1, θ_2 , and ϕ_{12} are shown in Fig. 1.7. In the second line of Eq. (1.2.10), we assume that $\mu = \mu_1 = \mu_2$.

This part of the pair potential is added mainly to account for the long-range interactions between the two molecules. It should be noted that the R^{-3} distance dependence of the dipole-dipole interaction is valid for fixed orientations of the dipoles. The *average* dipole-dipole interaction at large distance has an R^{-6} dependence.

The third contribution to the pair potential, U_{HB} , is the “hydrogen-bond” (*HB*) component of the interactions, which is more difficult to describe analytically. Qualitatively, U_{HB} should account for the *HB* interactions. We visualize a water molecule with four preferential directions, two along the O-H direction, and two along the “lone-pair” direction. These four preferential directions point to the four vertices of a regular tetrahedron (Fig. 1.9). Along the latter two (“lone-pair”) directions is a negative charge-concentration. When two water molecules are separated by a distance of about $R_{HB} \approx 2.76 \text{ \AA}$, and are oriented such that the O-H direction of one molecule is directed toward the lone-pair direction of the other, a hydrogen bond is formed (see the schematic description in Fig. 1.10). Fundamentally, a

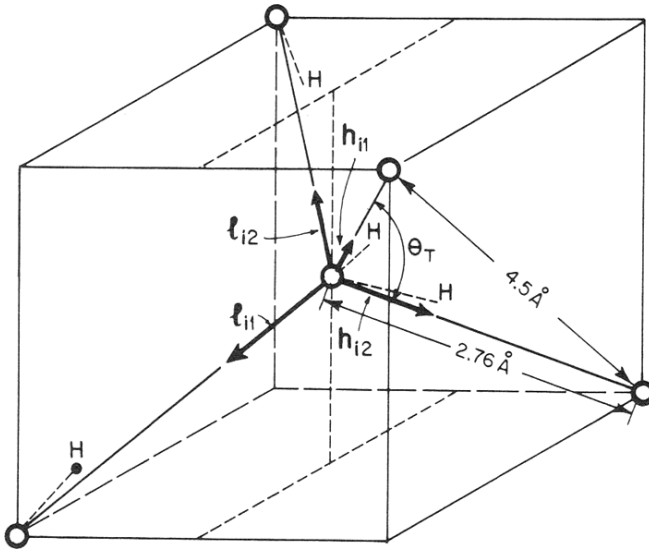


Fig. 1.9 Tetrahedral geometry (see the description in Sec. 1.2).

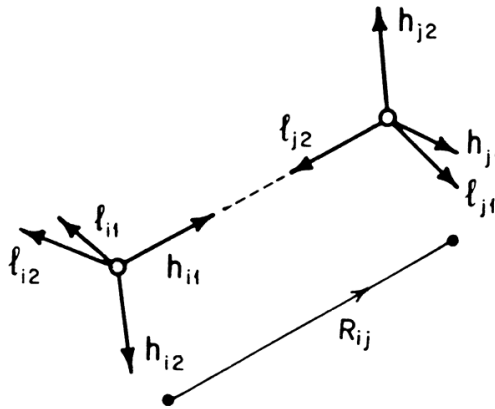


Fig. 1.10 A pair of water molecules in a configuration of a hydrogen bond.

hydrogen bond is a quantum-mechanical phenomenon,¹⁸ and our description of it here is only qualitative, but the important

¹⁸For an extensive discussion of hydrogen bonds, see Pauling (1959), Pimentel and McClellan (1960), or Marechal (2007).

thing to remember is that when two water molecules are oriented such that a hydrogen bond is formed; the interaction energy is quite large (of the order of $5\text{--}6\text{ kcal mol}^{-1}$).¹⁹ This interaction energy is an order of magnitude larger than that of a typical van der Waals interaction between two neon atoms, but an order of magnitude smaller than that of a typical covalent bond between two atoms within a molecule. (For instance, the O-H covalent bond energy is about 102 kcal mol^{-1} .)

It should be noted that tetrahedral geometry is not realized by a single water molecule. The ground state of an oxygen atom has the configuration $(1s)^2 (2s)^2 (2p)^4$. When forming a water molecule, the H-O-H angle is about 104.5° , slightly larger than the expected 90° from the perpendicular p-orbitals. This opening of the bond angle is ascribed to the repulsion between the two hydrogen atoms. The tetrahedral geometry is a result of the hybridization of the 2s and 2p orbital to form the sp^3 hybrid orbitals.

The “mechanism” for the formation of tetrahedral structures by water is similar to the formation of tetrahedral structures by carbon atoms. When a water molecule forms a hydrogen bond, the electron distribution around the oxygen atom changes. Four new orbitals are formed by the hybridization of the 2s and 2p orbitals of the oxygen atom. As a result of this hybridization, two lobes of charge are created by the unshared electron pairs (or lone-pair electrons), which are symmetrically located above and below the molecular plane. These two directions, together with the two O-H directions, give rise to the tetrahedral geometry, which is one of the most prominent structural features of the mode of packing of water molecules in the liquid and solid states.

¹⁹The linear configuration of the dimer as depicted in Fig. 1.10 has the lowest energy compared with other possible configurations of a dimer of water molecules.

It is convenient to introduce four unit vectors originating from the center of the oxygen atom and pointing toward the four corners of the regular tetrahedron (Fig. 1.9). Let \mathbf{h}_{ik} ($k = 1, 2$) be the two unit vectors belonging to the i th molecule and pointing approximately along the two O-H directions. The remaining two vectors \mathbf{l}_{ik} ($k = 1, 2$) are pointing along the directions of the lone pairs of electrons. Using the terminology of hydrogen-bond formation, we identify \mathbf{h}_{ik} as the directions along which molecule i forms a hydrogen bond as a *donor* molecule, whereas \mathbf{l}_{ik} is the direction along which the same molecule participates in a hydrogen bond as an *acceptor*. A simple geometrical consideration shows that the tetrahedral angle of $\theta_T = 109.46^\circ$ is obtained from the relation $\theta_T = \arccos(-1/3)$. For details, see Appendix A.

As mentioned above, because the pair potential for two water molecules [say, of the general form (1.2.7)] depends on six parameters, any calculation associated with the properties of water is extremely complex and time-consuming. For example, suppose we want to calculate an integral of the form

$$\int_a^b \{\exp[-\beta U(R)] - 1\} 4\pi R^2 dR \quad (1.2.11)$$

Here, $U(R)$ is a pair potential that depends only on distance R , β is a constant, $\beta = (k_B T)^{-1}$, and the integration extends from a to b . This kind of integral actually occurs in calculations of the pressure of a real gas. Here, we focus only on the technical aspect of the numerical calculation of this integral.

In order to perform a numerical integration, we divide the interval (a, b) into, say, 10 small intervals. We then calculate the area under the curve for each interval, as if it were a narrow rectangle, and then sum up all the areas obtained for each of these rectangles. As we increase the number of divisions of the interval a, b , we improve our estimation of the area under the curve.

Next, suppose we want to calculate an integral of the form (1.2.11), but with the pair potential for two water molecules. In this case, the potential function $U(R, \alpha_1, \alpha_2, \alpha_3, \alpha_4, \alpha_5)$ is a function of *six* parameters, one distance and five angles. We again choose only 10 points of divisions for each of the variables. This means that we have to evaluate the potential function at 10^6 points, instead of at only 10 points, as in the evaluation of the one-dimensional integral. This results in an exponential dependence of the computational time on the dimensionality of the pair potential and imposes a severe limitation on the accuracy of our calculations of the thermodynamic properties of water.

The pair potential is an important quantity that determines the deviations of the equation of state from the ideal gas equation of state. The equation of state of an ideal gas has the form

$$\rho = \frac{N}{V} = \frac{P}{RT} \quad (1.2.12)$$

where P is the pressure, R the gas constant, T the absolute temperature, and ρ the density of the gas.

The theoretical models of *ideal gases* presume the existence of non-interacting point particles. Such a system has an equation of state of the form (1.2.12). For *real gases* of interacting molecules, e.g. water, one can approximate the behavior of the system according to (1.2.12) provided that we take very low densities. How low? The answer depends on the specific molecules. The stronger the intermolecular forces, the lower the density is for which (1.2.12) holds true. For water, this low density ρ_w is much smaller than the low density ρ_A of argon. The reason is that, on average, two water molecules interact more strongly than two argon atoms. We must therefore take lower densities of water and hence, on average, larger intermolecular distances to obtain the ideal gas limiting behavior.

When we increase the density beyond the ideal gas limit, deviations from Eq. (1.2.12) are noticeable. In such cases one

can write correction terms to Eq. (1.2.12) that have the general form²⁰

$$\frac{P}{RT} = \rho + B_2(T)\rho^2 + B_3(T)\rho^3 + \dots \quad (1.2.13)$$

This equation gives the pressure of the gas as a function of the density. Clearly, when the density is very low, $\rho \rightarrow 0$, we have the limiting ideal gas behavior (1.2.12). At slightly higher densities, only the first correction to the ideal gas behavior should be taken into account, i.e. the equation of state at this density is

$$\frac{P}{RT} = \rho + B_2(T)\rho^2 \quad (1.2.14)$$

The coefficient $B_2(T)$ in the expansion (1.2.13) can be expressed as an integral over the pair potential. For spherical particles we have²¹

$$B_2(T) = -\frac{1}{2} \int_0^\infty \{\exp[-\beta U] - 1\} 4\pi R^2 dR \quad (1.2.15)$$

This result is one of the most remarkable achievements of statistical mechanics: it states that the first order deviations from an ideal gas behavior may be calculated from a system of exactly two molecules in a volume V and temperature T .

A similar expression may be written for more complicated pair-potential functions. A simpler form of the integral in Eq. (1.2.15) can be obtained for hard spheres of diameter σ , for which the potential function $U(R)$ is zero for $R \geq \sigma$, but infinite for $R < \sigma$ [see (1.2.9)]. Hence, the result of the integration is

$$B_2(T) = -\frac{1}{2} \int_0^\sigma (-1) 4\pi R^2 dR = \frac{2\pi\sigma^3}{3} = \frac{16\pi r_0^3}{3} \quad (1.2.16)$$

which is four times the volume of each hard sphere of radius r_0 .

²⁰The coefficients $B_2(T)$ and $B_3(T)$ depend on the temperature T , but not on the volume of the system.

²¹See, for example, Hill (1956).

The second virial coefficient for water may be written as²²

$$B_2(T) = -\frac{1}{2(8\pi^2)} \int d\mathbf{X}_2 f(\mathbf{X}_1, \mathbf{X}_2) \quad (1.2.17)$$

where f is defined by

$$f(\mathbf{X}_1, \mathbf{X}_2) = \exp[-\beta U(\mathbf{X}_1, \mathbf{X}_2)] - 1 \quad (1.2.18)$$

where \mathbf{X}_i is the vector comprising the six coordinates that are used to describe the configuration of a water molecule.

Figure 1.11 shows the values of $B_2(T)$ for water and heavy water. The two curves are almost indistinguishable on the scale of Fig. 1.11a. Figure 1.11b is an amplification of a part of Fig. 1.11a, in the region of lower temperatures.

Note also that for any substance at very high temperatures, the function f must tend to -1 ; hence, the second virial coefficient will tend to the value of the volume as in (1.2.16). As can

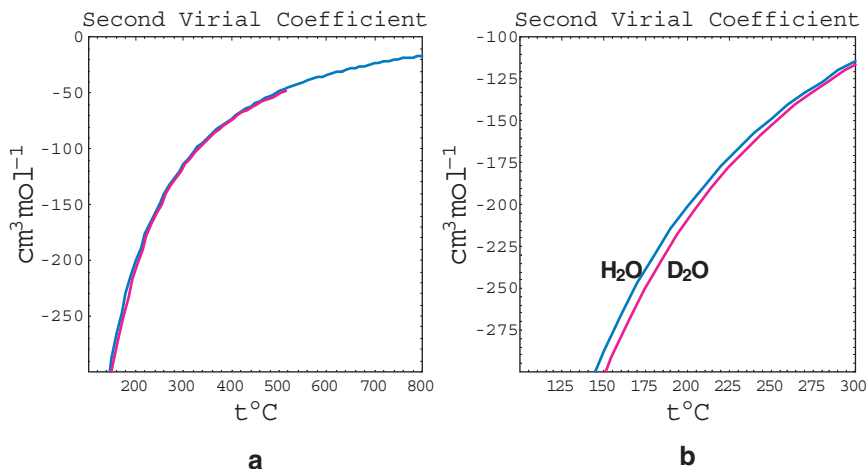


Fig. 1.11 Second virial coefficient for water and heavy water, based on data from Lemmon *et al.* (2007).

²²See, for example, Ben-Naim (1992).

be seen from Fig. 1.11, this limit is not reached at a temperature of 800°C.

The third virial coefficient $B_3(T)$ is more difficult to determine experimentally and far more difficult to compute. For a system with pairwise additive interactions, the third virial coefficient is expressed in terms of the pair potential as²³

$$B_3(T) = \frac{-1}{3(8\pi^2)^2} \int d\mathbf{X}_2 d\mathbf{X}_3 f(\mathbf{X}_1, \mathbf{X}_2) f(\mathbf{X}_1, \mathbf{X}_3) f(\mathbf{X}_2, \mathbf{X}_3) \quad (1.2.19)$$

Figure 1.12 shows the values of $B_3(T)$ for water and heavy water.

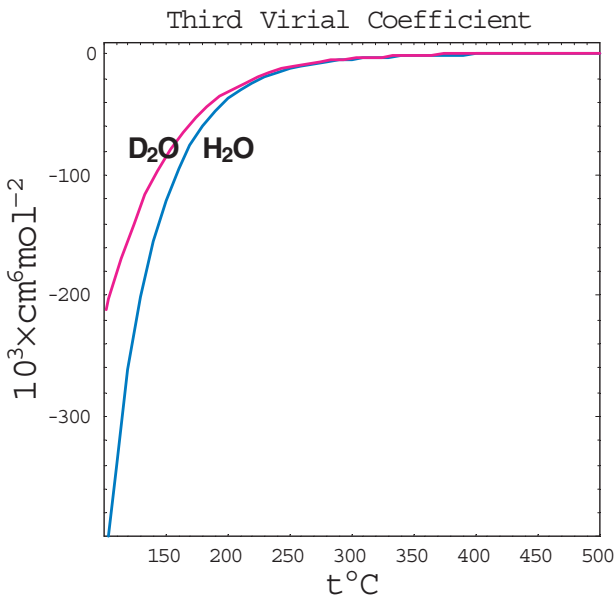


Fig. 1.12 Third virial coefficient for water and heavy water, based on data from Lemmon *et al.* (2007).

²³See, for example, Ben-Naim (1992).

Again, we note that in the high temperature limit,²⁴ $f \rightarrow -1$, and hence

$$B_3(T \rightarrow \infty) = \frac{1}{3} \left(\frac{4\pi\sigma^3}{3} \right)^2 \quad (1.2.20)$$

Before concluding this section it should be noted that in calculating the second virial coefficient, one needs the *true* pair potential for water. To study the properties of liquid water, or even the third virial coefficient, the *true* pair potential is not enough. The reason is that non-additive, higher order potentials are important in determining the properties of liquid water as well as of the third virial coefficient.

The extent of the non-additivity of the three-body potential is defined as the difference

$$\delta U_3 = U(\mathbf{X}_1, \mathbf{X}_2, \mathbf{X}_3) - U(\mathbf{X}_1, \mathbf{X}_2) - U(\mathbf{X}_1, \mathbf{X}_3) - U(\mathbf{X}_2, \mathbf{X}_3) \quad (1.2.21)$$

where $U(\mathbf{X}_i, \mathbf{X}_j)$ is the work done to bring two water molecules from infinite separation to the final configuration $\mathbf{X}_i, \mathbf{X}_j$. Similarly, $U(\mathbf{X}_1, \mathbf{X}_2, \mathbf{X}_3)$ is the work required to bring three water molecules to the final configuration $\mathbf{X}_1, \mathbf{X}_2, \mathbf{X}_3$.

A similar definition applies for four and higher order potential functions. For simple liquids, δU_3 is to a good approximation negligible. For water there is evidence that the additivity assumption of the higher order potentials is not justified.

The non-additivity of the *HB* was discussed qualitatively by Frank and Wen (1957),²⁵ and more quantitatively by Del Bene and Pople (1970) and Hankins *et al.* (1970). It was found that

²⁴Note that “high temperature” means high enough T such that $\beta U \rightarrow 0$ in regions where U is finite. For distances $R \leq \sigma$, $\beta U(R)$ is assumed to be infinity, or $\exp[-\beta U(R)] = 0$.

²⁵Frank and Wen use the term “cooperativity” of the hydrogen bonding to describe non-additivity.

the non-additivity of the hydrogen bonding is very significant.²⁶ We shall return to this question of non-additivity of the potential energy in Chapter 2.

1.3. Properties of Water in the Solid Phase

1.3.1. Ordinary ice

Ice can have at least nine different stable and well-characterized structures. The one referred to as “ordinary ice” is the one that we are all familiar with. This is obtained when water freezes at 0°C under ordinary atmospheric pressure. It is sometimes referred to as *hexagonal ice* and is denoted I_h .

The basic structure of ice was determined by Bragg in 1922 using the technique of X-ray crystallography. The “structure” of ice refers to the arrangement in space of the oxygen atoms. The structure of ordinary ice is shown in Fig. 1.13. The most important feature of the structure of ice is the *tetrahedral*

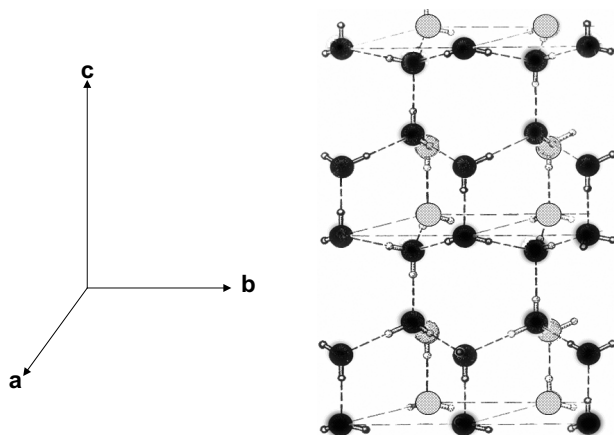


Fig. 1.13 The structure of ordinary ice I_h .

²⁶Hankins *et al.* (1970).

geometry: each oxygen atom is surrounded by four other oxygen atoms situated at the vertices of a regular tetrahedron, at a distance of 2.76 \AA from the central oxygen atom (see Figs. 1.9 and 1.13). As far as the geometry is concerned, the structure of D_2O is almost exactly the same as that of H_2O .

Suppose we shrink ourselves and sit at the center of an oxygen atom. We see four other oxygen atoms in our immediate vicinity, each one at a distance of 2.76 \AA and all four positioned in the four corners of a regular tetrahedron. This point of view does not reveal to us the entire three-dimensional structure of ice I_h . Take note that along the axis labeled c in Fig. 1.3, the oxygen atoms are arranged in a structural pattern that differs from the corresponding pattern of the oxygen atoms along the two axes perpendicular to c . The difference is shown in Fig. 1.14. If we look through an O-O nearest-neighbor bond along the c -axis, we see that all the other O-O bonds are “eclipsed,” i.e. on a 2-D drawing they would all be superimposed. On the other hand, if we look through an O-O bond along an axis (nearly) perpendicular to the c -axis, we see that three of the O-O bonds are rotated at an angle of 60° relative to the other three O-O bonds; this is the “staggered” configuration.

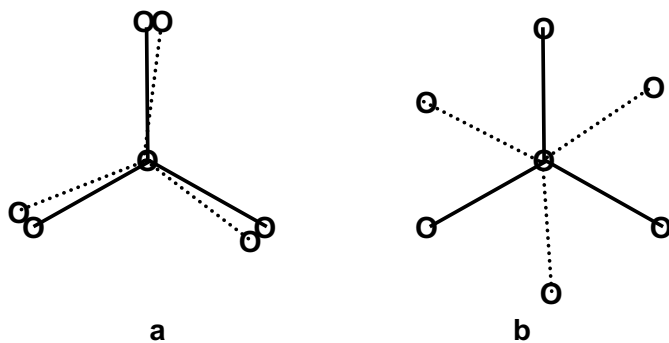


Fig. 1.14 Two views of the distribution of oxygens along the O-O axis: (a) eclipsed, and (b) staggered.

This difference in structure along different axes is revealed in the way the properties of ice differ according to the measurement along different axes. For example, the coefficient of linear expansion is $63 \times 10^{-6} \text{ } ^\circ\text{C}^{-1}$ along the *c*-axis but $46 \times 10^{-6} \text{ } ^\circ\text{C}^{-1}$ along an axis perpendicular to the *c*-axis (at -10°C). Similarly, the isothermal compressibility and the dielectric constant of ice are different along the different axes. For more details, see Eisenberg and Kauzmann (1969).

1.3.2. *The residual entropy of ice*

All the structural information discussed in the previous subsections is about the locations of oxygen atoms. Using X-ray crystallography, one cannot determine the locations of the hydrogen atoms.

In 1933, Bernal and Fowler concluded from the available experimental data that water molecules in ice maintain their molecular identity, and that the hydrogen atoms are located at the corners of a regular tetrahedron, the center of which is occupied by an oxygen atom. They formulated the so-called two ice conditions (see Fig. 1.15).

- (i) Each O-O line accommodates one and only one hydrogen atom.
- (ii) Each oxygen atom has two hydrogen atoms that are at a distance of about 1 \AA and two hydrogen atoms at a distance of about 1.76 \AA .

These two ice conditions reflect the experimental findings that when ice is formed from either the gas or the liquid phase, water retains its identity as a single molecule, i.e. one can identify single water molecules in the ice lattice. In addition, each pair of nearest-neighbor water molecules form hydrogen bonds in such a way that only *one* hydrogen is situated along the O-O

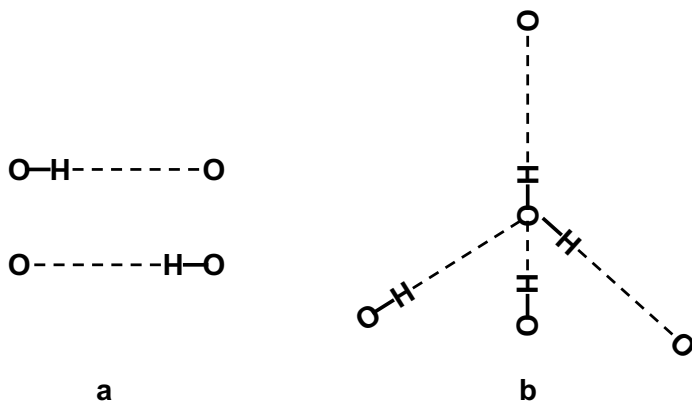


Fig. 1.15 The two ice conditions: (a) fulfilling condition (i), and (b) fulfilling condition (ii).

line (see Fig. 1.15). In this discussion of the structure of ice, we are disregarding the very small concentrations of ions such as OH^- and H_3O^+ . Such local defects do not conform to the ice conditions. Given the structural arrangement of the oxygen atoms, and assuming the validity of the two ice conditions, there is still a large number of possible arrangements for the hydrogen atoms.

In 1935, Pauling calculated the approximate number of possible configurations for the hydrogen atoms that are consistent with the ice conditions. This calculation is now considered a classical example of a successful prediction based on an elementary probabilistic argument. Because of its historical importance and its didactic simplicity, we present here Pauling's solution to this problem.

Consider a perfect ice structure containing N water molecules, i.e. N oxygen atoms are situated at N lattice points. The question is: How many ways can we arrange the $2N$ hydrogen atoms on this lattice such that the two ice conditions are fulfilled?

Since we are dealing with a macroscopic quantity of ice, N is of the order of the Avogadro number. Hence, we can neglect surface effects in our calculations.

For a very large crystal, N oxygen atoms produce $2N$, O-O nearest-neighbor bonds. We need to place the $2N$ hydrogen atoms in such a way that the two ice conditions are fulfilled. We first position the hydrogen atoms on the O-O bonds so that one hydrogen falls on each of the O-O bonds. Each O-O bond provides two locations for placing the hydrogen atom. These we denote O-H...O and O...H-O. In the first placement, the H is near the oxygen on the left-hand side; in the second, it is near the oxygen on the right-hand side. See Fig. 1.15a.

Since each of the hydrogen atoms can be placed at one of the two locations on the O-O bond, there are a total of 2^{2N} configurations that fulfill condition (i). Clearly, not all of the 2^{2N} configurations fulfill condition (ii). In Fig. 1.16, we show a system of five oxygen atoms and all of the possible arrangements of hydrogens around the central oxygen atom. Most of these configurations are not consistent with condition (ii). The next question is: How many of the 2^{2N} configurations are consistent with the second ice condition?

If we focus on a single oxygen atom and its four oxygen neighbors, we can make the following list of configuration types

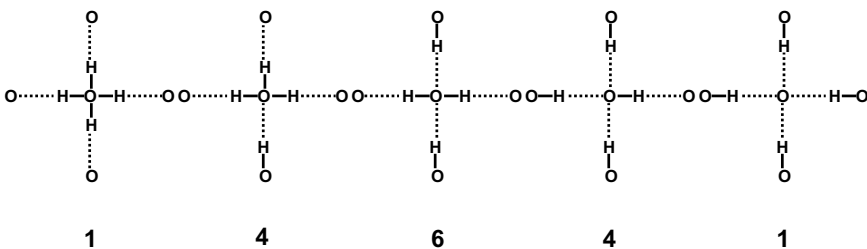


Fig. 1.16 The five possible arrangements of hydrogens around a given oxygen.

(see Fig. 1.16 from left to right):

- (1) One arrangement in which all hydrogens are close to the central oxygen.
- (2) Four arrangements in which three hydrogens are close to the central oxygen, while the other one is far away.
- (3) Six arrangements in which two hydrogens are close to the central oxygen, while the other two are far away.
- (4) Four arrangements in which one hydrogen is close to the central oxygen, while the other three are far away.
- (5) One arrangement in which all hydrogens are far away from the central oxygen.

Altogether, there are 16 different arrangements divided into five groups:

Group:	1	2	3	4	5
Number of arrangements:	1	4	6	4	1

Of these 16 arrangements, all of which are consistent with the first ice condition, only six arrangements (i.e. those in group 3) are also consistent with the second ice condition.

Pauling's reasoning is as follows: first assume that the fraction $6/16$ is also the *probability* of finding a single oxygen atom with the right configuration (i.e. one that fulfills the second ice condition),²⁷ and then assume that all oxygen atoms are

²⁷Note that this assumption is not exact. In the classical definition of probability, one calculates the probability of an event by taking the ratio of all configurations that are consistent with the event (here, 6), and dividing by the total number of configurations (here, 16). This method of calculating probability is valid only when all of the configurations are elementary events, i.e. when they all have an equal probability of occurring. It is not clear whether the 16 configurations in our case are elementary events.

independent.²⁸ The probability that all oxygen atoms have configurations that fulfill the second condition is therefore $(6/16)^N$. This is also the fraction of the total configurations that fulfill the two ice conditions. Hence, the number of the configurations that fulfill the two ice conditions is

$$\Omega = \left(\frac{6}{16}\right)^N 2^{2N} = \left(\frac{3}{2}\right)^N = 1.5^N \quad (1.3.1)$$

This result would not have been so remarkable had it not been related to the residual entropy of ice (see Appendix B).

The experimental value of the residual entropy of ice is known²⁹:

$$S_{\text{exp}} = 0.81 \text{ cal mol}^{-1}\text{K}^{-1} \quad (1.3.2)$$

Assuming that the residual entropy is determined by the number of configurations Ω in (1.3.1), we get the theoretical value of the residual entropy:

$$S_{\text{th}} = k_B \ln \Omega = k_B \ln (1.5)^N = R \ln 1.5 = 0.805 \text{ cal mol}^{-1}\text{K}^{-1} \quad (1.3.3)$$

The relation between S and Ω is the famous Boltzmann equation. It is engraved on Boltzmann's tombstone, which can be found in a Vienna cemetery. This is a very remarkable relation between a thermodynamic quantity (the entropy) on the one hand and the number of configurations of a system on the other. The larger the number of configurations (having equal probabilities), the larger the uncertainty, or the larger the missing information in the system. This is the essence of the

²⁸Again, from a mathematical point of view, independence exists only when the probability of occurrence of a particular configuration around a particular oxygen atom does not depend on the configuration around any other oxygen atom. It is not clear how valid this assumption is in the physical world of oxygen atoms in ice.

²⁹Giauque and Stout (1936). See also Di Marzio and Stillinger (1964) and Lebowitz (1968).

meaning of entropy. For more details, see Ben-Naim (2008). It is also a remarkable achievement that in spite of the drastic approximations made in calculating the number of configurations in (1.3.1), the experimental value of residual entropy of ice agrees quite well with the theoretical value based on Pauling's calculation.

Exercise 1.1. Calculate Ω by a different method. First, fulfilling condition (ii), then fulfilling condition (i).

The agreement between the experimental and the theoretical values of the residual entropy of ice clearly indicates that the distribution of hydrogen atoms within the ice lattice is not unique. There are many possible configurations that are consistent with the two ice conditions.

Note that to fulfill the second ice condition, we must maintain water molecules in ice as single entities, i.e. a pair of hydrogen atoms must “belong” to each oxygen atom. This does not mean that the structure of a single water molecule is the same as that of molecules in the gas phase. We recall that the H-O-H angle in a single water molecule in the gas phase is 104.5° . In a perfect ice crystal, the tetrahedral angle (a characteristic of a triplet of neighboring oxygen atoms O-O-O) is 109.5° , definitely larger than 104.5° .

1.3.3. *The phase diagram of water*

Figure 1.17 shows the phase diagram of water at low pressures. There are three regions denoted by: solid (I_b), liquid, and vapor. In each of these regions, one can change both the pressure P and the temperature T , and still observe only a single phase. For instance, suppose we start at point A in the figure, corresponding to a system of pure vapor. In this state, we have *two degrees of freedom*, i.e. we can change both the pressure P and the temperature T , and still observe a single pure phase. We can wander

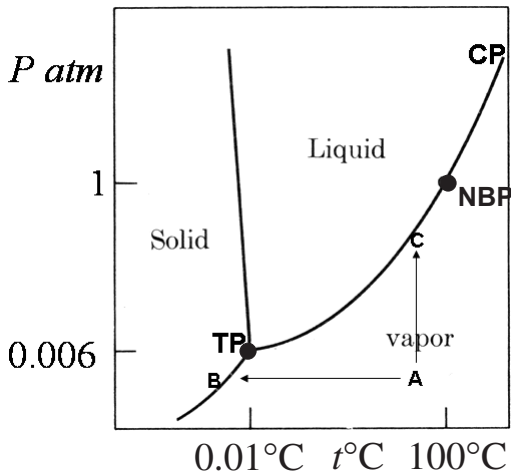


Fig. 1.17 The phase diagram of water at low pressures. The triple point (TP), the critical point (CP), and the normal boiling point (NBP) are indicated.

in each of these areas, i.e. changing independently both P and T , without encountering a new phase. However, when we reach one of the boundary lines, a new phase appears. For example, suppose we start at point A as above. As long as we make small changes in either P or T , we stay in the vapor area. If we keep the pressure fixed and decrease the temperature, we shall be moving along the line AB . As long as we do not hit the boundary line between vapor and solid, we have pure vapor. Once we reach point B , ice appears. The system now consists of two phases at equilibrium. The phase-rule of thermodynamics tells us that a system of two phases at equilibrium has only *one degree of freedom*. This means that we cannot change both P and T independently. Changing, for instance, the temperature, determines the pressure, i.e. we have the function $P = f_{VS}(T)$, which is the boundary curve between the vapor and the solid phases. Clearly, in this diagram, we have three such functions, one for the vapor-liquid boundary, one for the vapor-solid boundary, and one for

the liquid-solid boundary. Along each of these curves, there are two phases at equilibrium. As long as we change the temperature, as well as the pressure, in such a way that we “move” along one of these lines, we maintain the two phases at equilibrium.

Starting again at point *A*, keeping the temperature constant and increasing the pressure, we move along the *AC* line. As long as we do not hit point *C*, we observe one phase only, pure vapor. At point *C*, liquid appears and we observe two phases: liquid and vapor at equilibrium. Again, when we move along this line while maintaining the two phases, we must follow the corresponding function $P = f_{VL}(T)$, which describes the dependence between the two degrees of freedom P and T . Note that the three curves in this phase diagram are described by three different functions. We denote these functions by $f_{VL}(T)$, $f_{VS}(T)$, and $f_{SL}(T)$ for the vapor-liquid, vapor-solid, and solid-liquid phases, respectively.

Moving along any of the boundary lines, e.g. the vapor-solid line, we observe two phases at equilibrium. This is true until we reach a point, denoted *TP* in the diagram, at which a third phase appears. We now have three phases, vapor, liquid, and solid, at equilibrium. At this point, the phase-rule of thermodynamics tells us that there are *zero degrees of freedom*. In other words, we cannot “move” in the phase diagram while observing the three phases at equilibrium. The point at which the three phases exist at equilibrium is called the triple point (*TP*). This is a unique point in the phase diagram, and is characterized by $P = 0.006 \text{ atm}$ and $t = 0.01^\circ\text{C}$.³⁰

Note that since three phases are at equilibrium at the triple point, it must be the intersection of the three boundary lines. In other words, at the triple point, we have the equalities:

$$P_{TP} = f_{VL}(T_{TP}) = f_{VS}(T_{TP}) = f_{SL}(T_{TP}) \quad (1.3.4)$$

³⁰ $1 \text{ kbar} = 10^9 \text{ dyn cm}^{-2} = 986.9 \text{ atm}$.

In Fig. 1.17, we have noted one more unique point labeled *CP*. This is the vapor-liquid critical point. When we increase the temperature but follow the vapor-liquid boundary line, i.e. when we move along the curve $P = f_{VL}(T)$, we eventually reach a point where there is no distinction between the vapor and the liquid phases. The two phases become one. This point is characterized by the pressure $P_{CP} = 218 \text{ atm}$ and $T_{CP} = 374.15^\circ\text{C}$. The molar volume of the water at the critical point is $59.1 \text{ cm}^3 \text{ mol}^{-1}$.

Note that both the triple and critical points are uniquely defined in the phase diagram. They are fundamentally different kinds of points. The triple point, here of vapor-liquid-ice I_h , is characterized by the coexistence of three phases at equilibrium. On the other hand, when we approach the critical point along the vapor-liquid boundary line, the two phases become more and more similar — in the sense that the densities of the two phases become closer and closer. At the critical point, the densities of the vapor and the liquid phases become identical, and hence, we observe only a single phase. Beyond the critical point, i.e. increasing either the pressure, or the temperature, there exists only one phase which is referred to as a fluid. The fluid may be viewed as either a highly compressed gas or as an expanded liquid.³¹

If we move along the solid-liquid boundary, do we encounter a new critical point? The answer is no. We might encounter other triple points (see below) but never another critical point. The reason is that there exists a fundamental difference between a solid phase (any solid, not necessarily ice), and either a liquid or gaseous phase. Both the liquid and the gas phases are randomly disordered systems: the two phases differ in their densities. When we move along the vapor-liquid curve, the difference

³¹Recently, it was suggested that a “second critical point” might exist at temperatures below 0°C . See Stanley *et al.* (1998).

in the densities of the two phases become smaller and smaller until it disappears at the critical point. On the other hand, a solid is an ordered phase. When it is at equilibrium with either a gas or a liquid, there is a clear-cut distinction between the two phases. Order and disorder cannot gradually change until they are equal.

The slope of the two co-existing phases is obtained from the following considerations.

For two phases α and β at equilibrium, we have the equality of the chemical potentials of the two phases:

$$\mu_{\alpha}(T, P) = \mu_{\beta}(T, P) \quad (1.3.5)$$

Moving along the equilibrium line for two phases, the equality (1.3.5) must be maintained; hence

$$\begin{aligned} 0 &= d\Delta\mu = \left(\frac{\partial\Delta\mu}{\partial T}\right)_P dT + \left(\frac{\partial\Delta\mu}{\partial P}\right)_T dP \\ &= -\Delta S dT + \Delta V dP \end{aligned} \quad (1.3.6)$$

where $\Delta\mu = \mu_{\beta} - \mu_{\alpha}$. From (1.3.6), it follows that

$$\left(\frac{\partial P}{\partial T}\right)_{eq} = \frac{\Delta S}{\Delta V} \quad (1.3.7)$$

where $\Delta S = \bar{S}_{\beta} - \bar{S}_{\alpha}$ and $\Delta V = \bar{V}_{\beta} - \bar{V}_{\alpha}$ and the derivative is taken along the co-existing curve. This is the well-known Clapeyron equation. Since $\Delta\mu = \Delta H - T\Delta S = 0$, we can rewrite (1.3.7) as

$$\left(\frac{\partial P}{\partial T}\right)_{eq} = \frac{\Delta S}{\Delta V} = \frac{\Delta H}{T\Delta V} \quad (1.3.8)$$

Note that the slopes of the liquid-vapor and the solid-vapor are always positive. This is understandable; changing from a condensed phase (solid or liquid) to the vapor involves

an increase in entropy (or equivalently of enthalpy),³² and an increase in volume. Therefore, the right-hand side of (1.3.8) is always positive.

In most substances the solid-liquid curve has a positive slope too, for the same reason given above. Water is anomalous as can be seen from Fig. 1.17: the slope of the solid-liquid curve is negative. This means that ΔH and ΔV have *different* signs. This is an important observation. We shall discuss its molecular implications in the next chapter.

Most substances have a phase diagram similar to that of Fig. 1.17. They differ in their triple point and critical point locations, and of course in the location of the boundaries between phase pairs.

Water has at least eight well-defined solid phases. Figure 1.18 shows the phase diagram of water. There are some metastable forms not shown in the figure. Note that the entire phase diagram of Fig. 1.17 is not even seen in Fig. 1.18. The reason is simple. The triple point of water (i.e. ice I_h , liquid, and vapor) is at a pressure of less than 1 atm. Even the critical point has a pressure of 218 atm. The units of pressures in Fig. 1.18 are in kbars (about 1000 atm). This means one kbar is already far higher than the critical point of water. In the phase diagram of Fig. 1.18, the boundary lines are either between the liquid and one solid phase, or between two solids of different crystalline structures. Note that there are several triple points, each representing three phases at equilibrium. In this phase diagram we see seven triple points. Four of these include liquid water, and two solid forms, and three include only solid forms at equilibrium (the triple point of ice I_h , liquid-vapor, is not seen in this figure).

³²The increase in entropy is traditionally interpreted as an increase in *disorder*. However, one does not need to invoke *disorder* to explain $\Delta S > 0$. Since $\Delta H = T\Delta S$, one can interpret the positive change in entropy as a positive change in enthalpy, which is basically a change in energy.

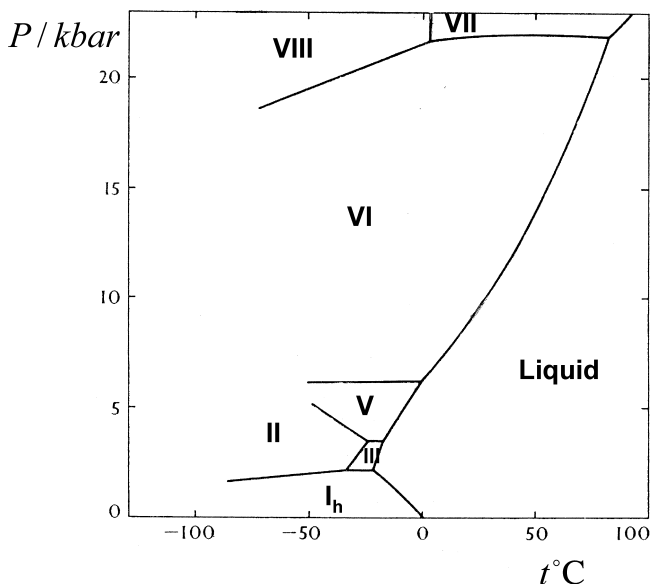


Fig. 1.18 The phase diagram of the various forms of ice.

Much work has been done to characterize the structure and properties of all the ice polymorphs. For the purpose of understanding liquid water and its role in biological systems, one does not need to know the details of the high pressure forms of ice. There is one property worth noting, however, which is relevant to the study of liquid water. This has to do with the densities and lattice energies of the high pressure ices.

When we cross the boundary line between ice I_h to ice II, the volume *decreases* by about $3.92 \text{ cm}^3 \text{ mol}^{-1}$ and the internal energy *increases* by 19 cal mol^{-1} . Furthermore, crossing the boundary between ice II and ice V, there is an additional *decrease* in volume of about $0.7 \text{ cm}^3 \text{ mol}^{-1}$, but an *increase* in internal energy of 347 cal mol^{-1} . Crossing from ice V to ice VI causes a further *decrease* in the volume of $0.7 \text{ cm}^3 \text{ mol}^{-1}$, and an *increase* in the internal energy of 101 cal mol^{-1} . Finally, crossing from ice VI to ice VII causes a *decrease* of about $1.05 \text{ cm}^3 \text{ mol}^{-1}$ in

volume, and an *increase* in energy of 550 cal mol^{-1} . Note that all these slopes are relatively small compared with transitions such as VII \rightarrow VIII. Some of these changes involve a change in the ordering of hydrogen atoms. For more details, see Eisenberg and Kauzmann (1969).

At first glance these findings are puzzling. The high pressure polymorphs have a higher density (or lower molar volume). A higher density means that, on average, each water molecule is surrounded by a larger number of neighbors. Normally, a larger number of neighbors implies a stronger interaction energy between a molecule and its surroundings.³³ A stronger interaction energy should increase the (absolute) internal energy (i.e. make it more negative) of the entire solid. The actual finding in the ice polymorphs is that in some cases increasing the densities causes an increase in internal energy (i.e. makes the internal energy *less* negative) in spite of the fact that each water molecule interacts with a larger number of neighbors.

A variety of interesting properties are manifested by the high pressure polymorphs of ice. For details, see Fletcher (1970) and Eisenberg and Kauzmann (1969). For the purpose of the study of liquid water, it is useful to remember that a large number of structures can be formed around a water molecule in the solid state. In particular, we draw attention to the fact that both open and close-packed structures are possible. There is no doubt that the open structure of ice, I_h , is maintained because of strong directional forces (hydrogen bonds) operating along the directions of the four unit vectors, as depicted in Fig. 1.9. The high pressure polymorphs of ice are characterized by relatively higher densities. That is, each water molecule experiences a higher local

³³This is true as long as the pressure is not so high that the molecules are pushed into intermolecular distances shorter than their molecular diameters.

density than in ice I_h . In spite of the fact that the number of nearest neighbors is larger in some of these structures, their internal energies are higher than those of ice I_h , which indicates that the average binding energy of a water molecule in an open structure may be stronger than the binding energy of the same molecule in a more closely packed structure.³⁴ We will see later that the relation between local density and binding energy is the most important aspect of the mode of packing of water molecules in the liquid state. It is so important that I have chosen to depict this principle in the cover design for this book.

1.4. Properties of Water in the Liquid Phase

In this section, we shall survey some of the outstanding properties of liquid water. We shall discuss only equilibrium thermodynamic quantities. Sometimes these properties are referred to as *anomalous* properties or *unique* properties. We shall occasionally use these terms as well as the term *outstanding*, in describing those properties of liquid water that differ considerably from the values of the same properties in other liquids. To claim uniqueness is not always justified unless one examines the properties of *all* other liquids and find that water has indeed a unique property.³⁵ Recently, Angell *et al.* (2000) concluded that water's position "is not one of extreme anomaly as often supposed but rather one of intermediate status." It should be noted that supercooled water shows some anomalies, both experimentally and in simulation. It was also postulated that there exists a "second critical point" in the supercooled region (Stanley *et al.* 1998). For a review, see Lang and Ludermann (1982)

³⁴It should be noted that, in general, higher local density can be achieved by either more neighbors or by the same number of neighbors but at closer distances.

³⁵Recently, Agarwal *et al.* (2007) showed that beryllium difluoride exhibits some properties similar to liquid water.

and Angell *et al.* (2000). An interesting discussion of the various anomalies of liquid water was published very recently by de Oliveira *et al.* (2006).

1.4.1. *Some outstanding properties of water*

Consider the following series of substances: methane (CH₄), ammonia (NH₃), water (H₂O), hydrofluoric acid (HF), and neon (Ne). These substances are all isoelectronic, i.e. they all have 10 electrons (hence also 10 protons — since the molecules themselves are electro-neutral).

Table 1.4 shows the values of the melting point (in °C), the boiling point (in °C), and the heat of evaporation (in cal mol⁻¹) of each of these substances. Looking at each of these three columns we notice that the values first increase, then sharply decrease — and that the maximal value is attained by liquid water. The same information is also shown graphically in Fig. 1.19, where, in addition to the series of substances reported in Table 1.4, we have a series of compounds of the general formula RH_{*n*}, where *R* is a varying atom down a column of the periodic table of the elements and *n* is the number of hydrogens in the compound.

Consider the series of CH₄, SiH₄, GeH₄, and SnH₄. We see that in this homologous series, the properties change “regularly”

Table 1.4. Some Physical Properties of a Series of Isoelectronic Substances

Substance	Melting Point (°C)	Boiling Point (°C)	Molar Heat of Vaporization (cal mol ⁻¹)
CH ₄	-184	-161.5	2200
NH ₃	-78	-33.4	5550
H ₂ O	0	+100	9750
HF	-92	+19.4	7220
Ne	-249	-246	415

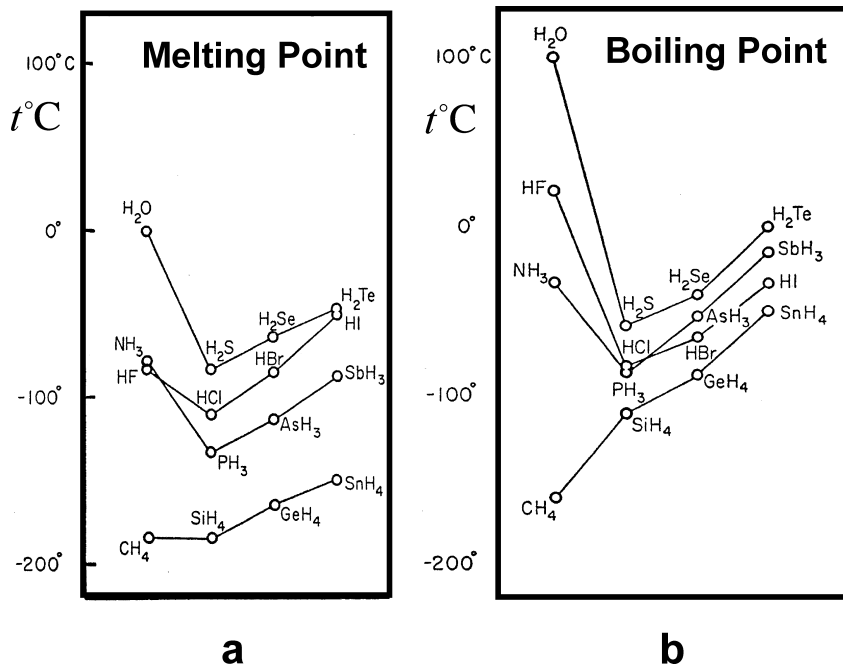


Fig. 1.19 (a) The melting points and (b) boiling points of isoelectronic sequences of hydride molecules [redrawn from Pauling (1960)].

with the molecular weight, or with the size of the molecule. Note that the ordinates in these figures report the numerical values of the melting points and the boiling points. The abscissa, on the other hand, indicates only the row in the periodic table from which the element R in RH_4 has been taken. From this series one can conclude that the larger the molecular weight of the substance, the higher the melting and boiling temperatures.

We see clearly that the properties of the substances HF, H₂O, and NH₃ have high values — far above the values that we would have derived if we extrapolated from the values of the same property of the homologous substance. This is most conspicuous for the homologous substances H₂O, H₂S, H₂Se, and H₂Te.

Although the last three compounds roughly form a straight line with increasing values from H_2S to H_2Se to H_2Te , the value of water is outstandingly high.

The high values of the melting points, the boiling points, and the heat of vaporizations of H_2O , NH_3 , and HF can all be explained by introducing the concept of hydrogen bonding. This was qualitatively explained by Pauling in his classic book, "The Nature of the Chemical Bond," first published in 1939. Basically, the hydrogen bond is not a chemical bond in the usual sense. Although a hydrogen atom can form only one pure covalent bond, a hydrogen *ion* H^+ — with its small radius — exerts a strong electrostatic force that attracts simultaneously two electro-negative atoms, such as oxygen atoms. Figure 1.20 shows how the small proton H^+ can bring two relatively large negative ions (denoted A_1^- and A_2^-) in close proximity. As can be seen in Fig. 1.20, a third ion (denoted A_3^-) approaching this pair cannot come close to the proton. Hence, effectively, the hydrogen ions act as a "glue" that binds no more than two negative ions together. This type of "saturation" is typical in a chemical bond and can be observed in all hydrogen bonds.

It has also been found that the greater the electro-negativity of the ions, the stronger the hydrogen bonds. Fluoride ions form

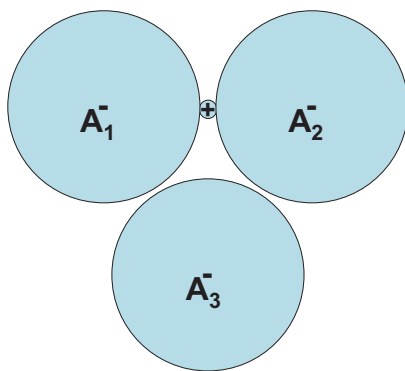


Fig. 1.20 Schematic description of the electrostatic interaction in hydrogen bonding.

very strong hydrogen bonds, oxygen forms somewhat weaker hydrogen bonds, nitrogen forms still weaker hydrogen bonds, and carbon almost does not form hydrogen bonds.

Note that although the strength of a single hydrogen bond increases from nitrogen to oxygen to fluoride, the effect of hydrogen bonding is more dramatic in water than in hydrofluoric acid. The reason is that in liquid water a water molecule can form up to *four* hydrogen bonds with its neighboring molecules.

Viewing the phenomenon of hydrogen bonding as a force of adhesion between water molecules in the liquid state, we can immediately understand the high values of the melting point, boiling point, and heat of vaporization. Since the forces that hold water molecules together are strong, a relatively high temperature is needed to melt ice. Note that we are comparing the melting point of pure water with the melting points of only those substances shown in Fig. 1.19. There are many other substances with much stronger binding forces, and hence higher melting points. Table 1.5 shows the values of melting points and boiling points of H₂O, D₂O, and T₂O. The larger values of both the melting points and the boiling points of D₂O and T₂O indicate stronger interaction energies among D₂O and T₂O molecules compared with H₂O.

Throughout the entire liquid range of temperatures; 0°C to 100°C, the average number of hydrogen bonds decreases as the temperature increases. However, even at the boiling point, there are many water molecules still engaged in hydrogen bonding.

Table 1.5. Melting and Boiling Points of Various Liquids

	Melting Point (°C)	Boiling Point (°C)
H ₂ O	0.00	100
D ₂ O	3.82	101.42
T ₂ O	4.49	101.51

Table 1.6. The Entropy of Vaporization Divided by the Gas Constant R for Various Liquids

Substance	$\Delta S_v/R$
Ar	9.0
Kr	9.1
Xe	9.2
CH ₄	8.8
H ₂ S	10.6
NH ₃	11.7
CH ₃ OH	12.6
CH ₃ CH ₂ OH	13.2
H ₂ O	13.1

To detach water molecules from the liquid and to send them into the gaseous phase, one needs more energy, which explains the relatively higher boiling temperature of water and high value of the heat of vaporization.

An empirical law known as Trouton's Law says that the entropy of vaporization is almost constant, about $20.3 \text{ cal mol}^{-1} \text{ K}^{-1}$. Water has an anomalously large entropy of vaporization of about $26 \text{ cal mol}^{-1} \text{ K}^{-1}$. Table 1.6 shows the entropy of vaporization divided by the gas constant R for different liquids. Note that the entropy of vaporization of ethanol is as large as that of water.

1.4.2. *Molar volume of water and its temperature dependence*

Among the other unusual properties of pure liquid water, one of the best known is the way water expands when it freezes.³⁶ Never put a bottle filled with water inside the freezer. It will

³⁶The molar volumes of water and ice at the normal freezing points are 18 and $19.6 \text{ cm}^3 \text{ mol}^{-1}$, respectively.

explode upon freezing. This is quite an unusual phenomenon (though not entirely unique to water; there are other substances that also have a larger molar volume in the solid state compared to the liquid state). The molecular reason for this phenomenon is clear. It is due to the “open” mode of packing water molecules in ordinary ice.

An even more unusual property, one which is unique to liquid water is the continual decrease of the molar volume of water upon increasing the temperature between 0°C to 4°C (for heavy water, D₂O, up to 11°C); see Fig. 1.21.

The expansivity of a substance is defined by

$$\alpha_p = \frac{1}{V} \left(\frac{\partial V}{\partial T} \right)_p \quad (1.4.1)$$

where V is the volume of the system, and the derivative is taken with respect to the temperature, keeping the pressure constant. Figure 1.21 shows the temperature dependence of the volume of water, heavy water and for comparison also for methanol and ethanol (Fig. 1.21c).

All known liquids expand upon increasing the temperature, whereas liquid water between 0°C and 4°C shows the opposite behavior. Note also that D₂O has a larger molar volume in the entire range of temperatures. The locations of the minimum volume are indicated in Fig. 1.21b. This phenomenon is also due to the mode of packing water molecules in such a way that low local density is correlated with strong binding energy. We shall discuss this principle in great detail in Chapter 2. We shall see that the understanding of this phenomenon at a molecular level is essential to the understanding of some of the outstanding properties of aqueous solutions.

Figure 1.22 shows that as we increase the pressure, the minimum of the volume is shifted to lower temperatures. At

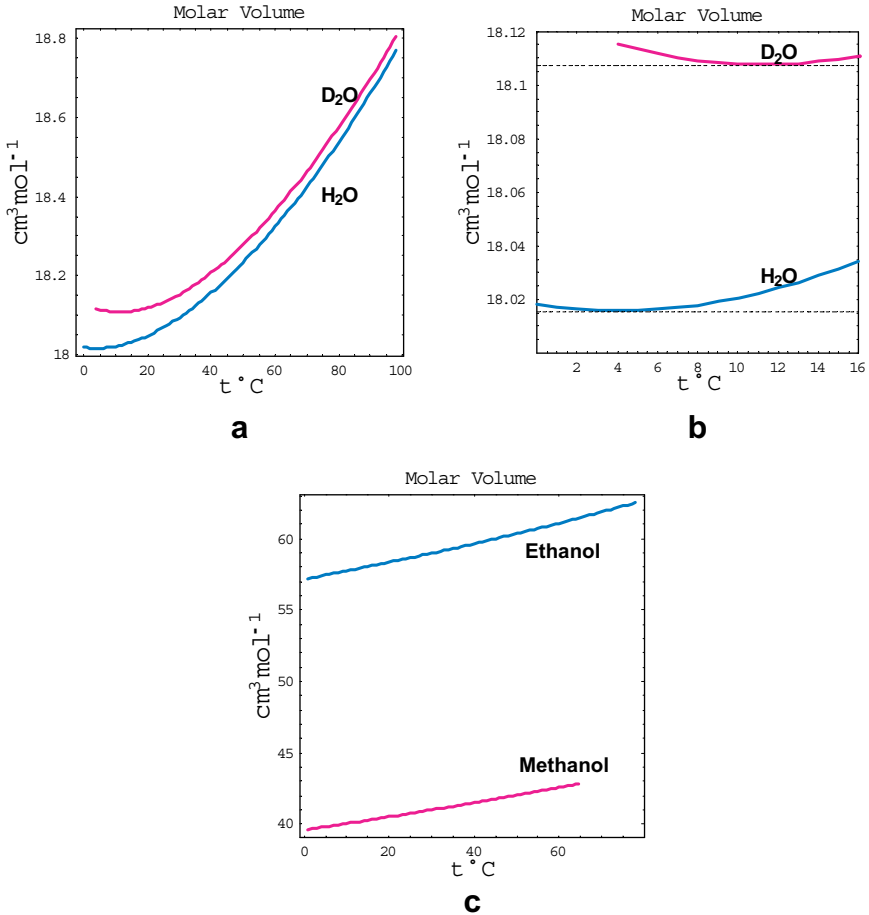


Fig. 1.21 The temperature dependence of the molar volume of (a) water and heavy water, (b) A magnified figure near the minimum of the volume, and (c) methanol and ethanol.

higher pressures the minimum disappears and water behaves as a normal liquid.

1.4.3. Heat capacity

The heat capacity is defined as the amount of heat required to raise the temperature of one mole of a substance by one degree.

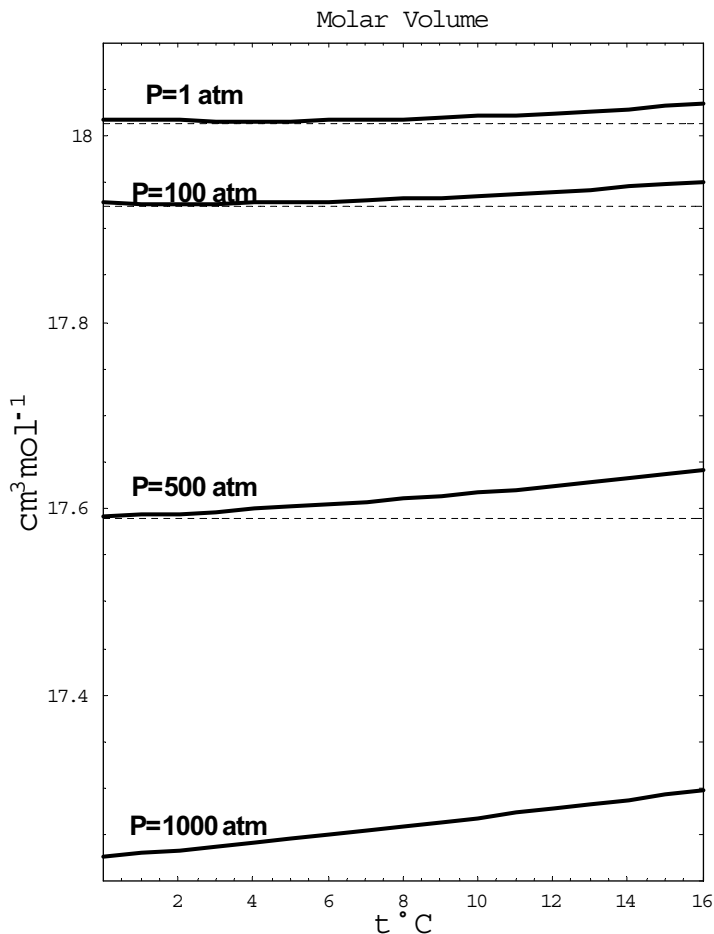


Fig. 1.22 The temperature dependence of a volume of water at different pressures.

The value of the heat capacity depends on the conditions in which the experiment is carried out. The most commonly used heat capacities are:

$$C_V = \left(\frac{\partial E}{\partial T} \right)_V, \quad C_p = \left(\frac{\partial H}{\partial T} \right)_P \quad (1.4.2)$$

where E is the internal energy of the system and H is the enthalpy of the system.

The heat capacity of water is much larger than that of other normal liquids. For example, the heat capacity of water at 25°C is about $1 \text{ cal g}^{-1} \text{ K}^{-1}$. For ethanol, it is $0.6 \text{ cal g}^{-1} \text{ K}^{-1}$, and for hexane, $0.6 \text{ cal g}^{-1} \text{ K}^{-1}$, but for ammonia, it is $1.23 \text{ cal g}^{-1} \text{ K}^{-1}$. When we say large, we mean larger than the value that is expected from a regular non-hydrogen bonded fluid. Note that in both the solid and the gaseous phases, the value of the heat capacity is “normal,” i.e. it is consistent with what one would calculate from statistical thermodynamics. In the liquid phase, however, the value of the heat capacity is almost three times larger than expected.

Figure 1.23 shows the values of the heat capacity C_P as a function of T for H_2O , D_2O , and for comparison also for ethanol and methanol. Figure 1.24 shows the heat capacity C_V for the same four liquids. Note that the curve of C_P for H_2O goes through a minimum at about 35°C . For D_2O there seems

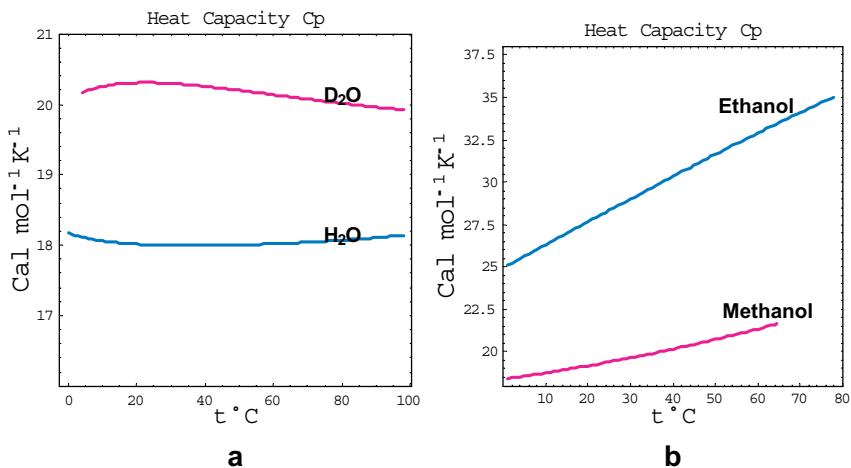


Fig. 1.23 Heat capacity C_P of (a) H_2O , D_2O , and (b) ethanol and methanol as a function of temperature T at $P = 1 \text{ atm}$.

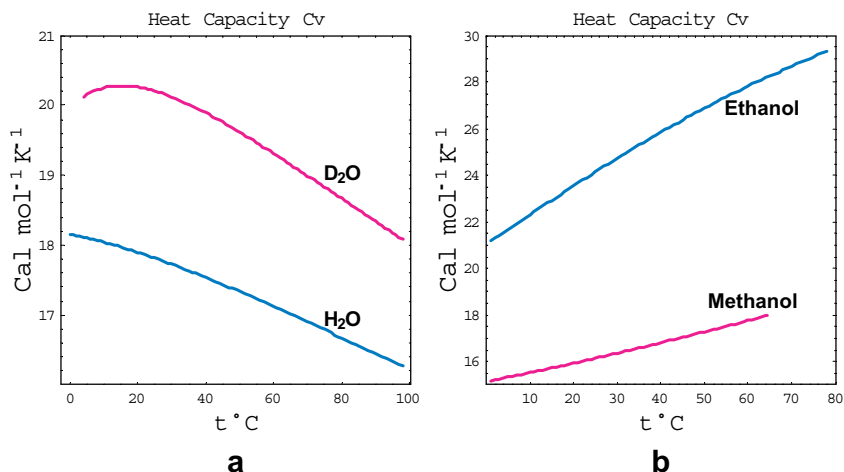


Fig. 1.24 Heat capacity C_V of (a) H_2O , D_2O , and (b) ethanol and methanol as a function of T at $P = 1$ atm.

to be a maximum of both C_V and C_P around 20°C . Note that the high value of the heat capacity is not unique to liquid water. Other liquids such as ammonia also have high heat capacity. The molecular interpretation of these quantities will be discussed in Chapter 2.

Figure 1.25 shows that when we increase the pressure, the heat capacities become smaller and the minimum disappears; again, the behavior of a normal liquid.

1.4.4. Isothermal compressibility

The isothermal compressibility of water, denoted κ_T , is a measure of the response of the volume of a liquid to increasing the pressure.³⁷ This is defined by

$$\kappa_T = -\frac{1}{V} \left(\frac{\partial V}{\partial P} \right)_T = \left(\frac{\partial \ln \rho}{\partial P} \right)_T \quad (1.4.3)$$

³⁷Some refer to the isothermal compressibility as a “response function.” This is true, but it is true for any derivative with respect to P , T , or N .

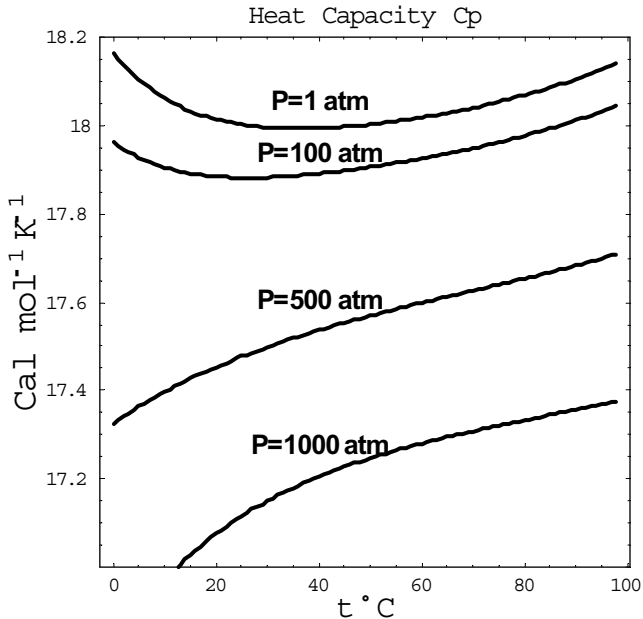


Fig. 1.25 The heat capacity C_p of water as a function of temperature at different pressures.

Normally, as the temperature of a liquid increases the average intermolecular distance between the particles of the liquid increases. This makes it easier to compress a liquid at a higher temperature. Thus, we expect the compressibility to increase as we increase the temperature. Water is anomalous in that it has a region below approximately 45°C, where κ_T actually decreases as the temperature increases (Fig. 1.26). At 45°C, the compressibility passes through a minimum, and thereafter it increases with T , as in the case of normal liquids.

Figure 1.27 shows the temperature dependence of the compressibility curves at different pressures. As can be seen from Fig. 1.27, when we increase the pressure, the minimum in the compressibility becomes less and less pronounced, but even at 3000 atm we still observe a shallow minimum.

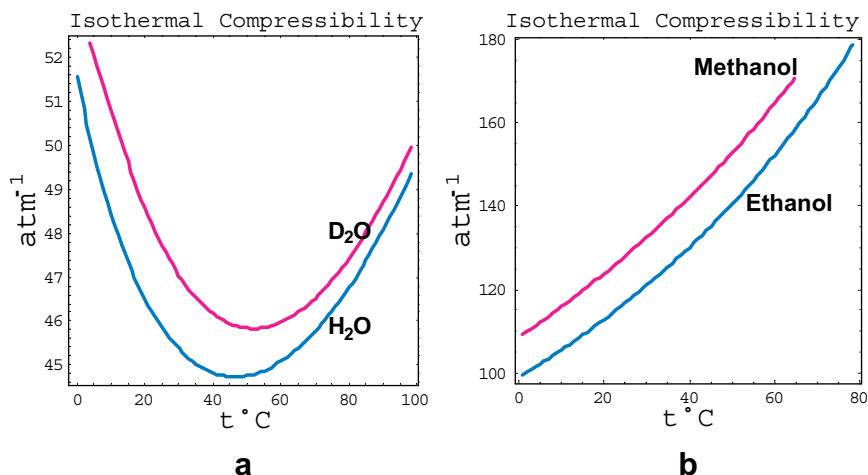


Fig. 1.26 The isothermal compressibility κ_T as a function of T for (a) H_2O , D_2O , and (b) ethanol and methanol as a function of T at $P = 1$ atm.

Table 1.7 shows the isothermal compressibilities of some liquids at $P = 1$ atm. Note that water has a relatively small value of compressibility. However, the isothermal compressibility of glycerol at 28°C is even smaller: $21.1 \times 10^{-6} \text{ atm}^{-1}$.

Liquid water has many other properties that exhibit anomalous values, e.g. dielectric constant, surface tension, diffusion coefficient, viscosity, etc. Aqueous solutions also exhibit unusual properties, some of which will be discussed in Chapter 3. In this introduction, we have mentioned only a few properties, the interpretation of which can be given by some simple theoretical arguments. We shall discuss these properties again in Chapter 2.

1.4.5. The radial distribution function of water

The most important experimental information on the mode of packing of water molecules in the liquid state is contained in the radial distribution function, which is obtained from X-ray

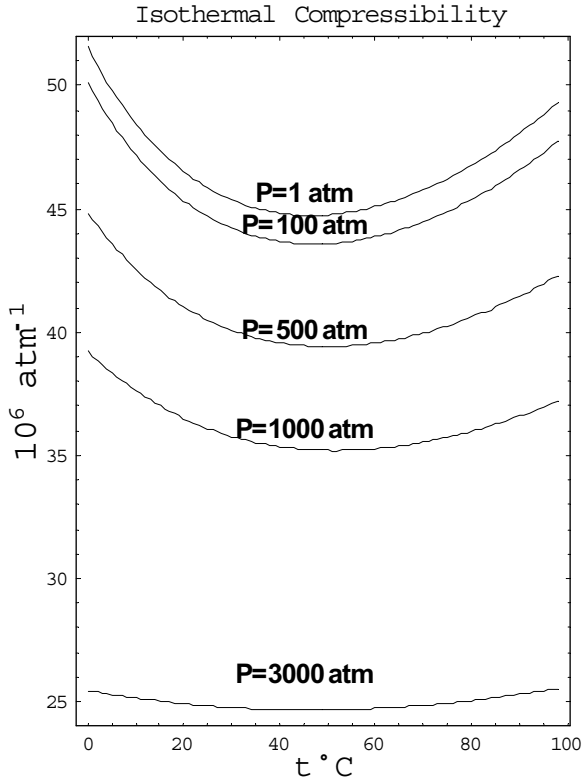


Fig. 1.27 The isothermal compressibility of water as a function of T for various pressures.

or neutron scattering data. A solid is characterized by a well-defined structure: the molecules are packed in some orderly fashion. The liquid phase, on the other hand, seems to be lacking any structure. Nevertheless, it is possible to detect some regularities in the packing mode of the molecules in the liquid phase.

If we could sit at the center of one of the particles and observe our surroundings, we would not see any regular pattern that we could call a “structure.” But if we counted the number of particle centers that appeared within a spherical shell of width dR at a distance R , we would find the following regularities.

Table 1.7. Isothermal Compressibilities of Water and Some Alcohols

	t ($^{\circ}\text{C}$)	$\kappa_T \times 10^6 \text{ atm}^{-1}$
H ₂ O	20	45.91
	25	45.52
Methanol	20	121.4
Ethanol	20	111.9
Acetone	20	126.2
Ethyl acetate	20	113.2
Ethylene glycol	20	36.4
Glycerol	28	21.1

Each spherical shell of width dR at a distance R has a volume $4\pi R^2 dR$. If the average (or macroscopic) density of the liquid is $\rho = N/V$, then we would expect to find, on average, $\rho 4\pi R^2 dR$ particle centers within this volume. However, because our vantage point is located at the center of a specific particle, we observe an average density that deviates from the expected density ρ . We define a function $g(R)$ in such a way that the actual average density at a distance R from the center of a specific particle is $\rho g(R)$. Equivalently, the average number of particles in each spherical shell is $\rho g(R) 4\pi R^2 dR$, not $\rho 4\pi R^2 dR$. Thus, $g(R)$ is a measure of the deviation of the actual count of the average number of particles around a given particle, relative to the average number of particles that we should expect to find in a spherical shell of radius R centered at a *random* point in the liquid. The function $g(R)$ is referred to as either the pair correlation function or as the radial distribution function (RDF).

Having this qualitative definition of $g(R)$, we now turn to describing some of its salient features for spherical particles:

- (i) If σ is the diameter of each particle in the system, then the probability of finding any other particle at a distance of less

than σ from a given particle is almost zero, i.e.

$$g(R) \approx 0 \quad \text{at } R \leq \sigma \quad (1.4.4)$$

The reason for this is that at distances $R \leq \sigma$, the two particles exert strong repulsive forces; hence, they are effectively impenetrable. (In fact, the diameter σ is *defined* as the distance below which the repulsive forces are so large that the two particles practically cannot approach each other to a distance shorter than σ .)

- (ii) At a very long distance $R \rightarrow \infty$, we expect that the average number of particles in the element of volume dV will not depend on the fact that we have placed a particle at the origin of our coordinate system. Therefore, we expect that the average number of particles in the spherical shell around the center of a specific particle to be the same as $\rho 4\pi R^2 dR$. We say that as R becomes very large, there exists no *correlation* between the particles. Clearly, in this case $g(R) \approx 1$, for $R \rightarrow \infty$. We have written $R \rightarrow \infty$ to signify that R is a very large distance. In practice, for regular liquids not close to their critical point, one finds that the correlation function is very close to unity (i.e. that there is no correlation) when R is approximately five or six times the molecular diameter of the particles (see Fig. 1.28).
- (iii) At distances $\sigma \lesssim R \lesssim 4\sigma$, we find (both experimentally and from theoretical calculations) that $g(R)$ has, in general, successive maxima and minima, as is shown in Fig. 1.28. Note that the first maximum occurs at about $R \approx \sigma$, the second maximum at $R \approx 2\sigma$, and the third at $R \approx 3\sigma$. Each time we increase R , the value of the maximum decreases from $g(R \approx \sigma)$ to $g(R \approx 2\sigma)$, to $g(R \approx 3\sigma)$. For $R \approx 4\sigma$ or $R \approx 5\sigma$, the value of $g(R)$ becomes practically unity, i.e. there is almost no correlation beyond, say, $R \approx 5\sigma$.

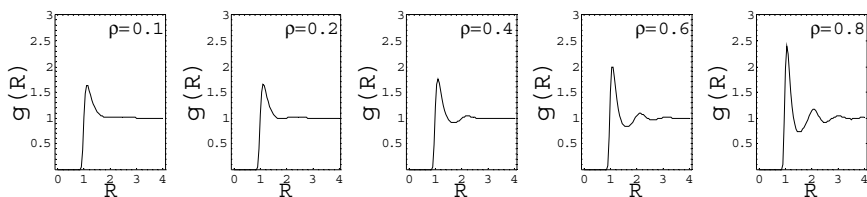


Fig. 1.28 Dependence of $g(R)$ on the density of the system. The corresponding (number) densities are indicated in each figure. The functions $g(R)$ for these illustrations were computed using a numerical solution to the Percus–Yevick equation for Lennard–Jones particles with parameters $\sigma = 1.0$ and $\epsilon/k_B T = 0.5$.

(iv) In Fig. 1.28, we see that more maxima and minima appear as the density of the liquid increases. At very low densities, there is only one maximum (left-hand curve in Fig. 1.28). This is the limit of $g(R)$ as $\rho \rightarrow 0$. At this limit, $g(R)$ is determined only by the pair potential. The relation between the two is: $g(R) = \exp[-\beta U(R)]$. Note that $\rho \rightarrow 0$ is the low density limit of a *real* liquid. A *theoretical* ideal gas is a system containing only non-interacting particles. For such particles, $g(R) \approx 1$, i.e. whatever the distances and densities in the system, correlations between the particles are never present.

The typical concentric and approximately equidistant peaks observed in $g(R)$ are a result of the spherical-symmetrical interaction between the particles. This information provided by $g(R)$ is sometimes called the “structure” of the liquid, but when applied to liquid water $g(R)$ is not a good measure of structure.

Figure 1.29b shows the first two distances σ and 2σ , where one can expect to find a peak in the pair correlation function for spherical molecules. For non-spherical molecules such as water, the pair correlation function is a function of both the distance and the relative orientation of the pair of molecules.

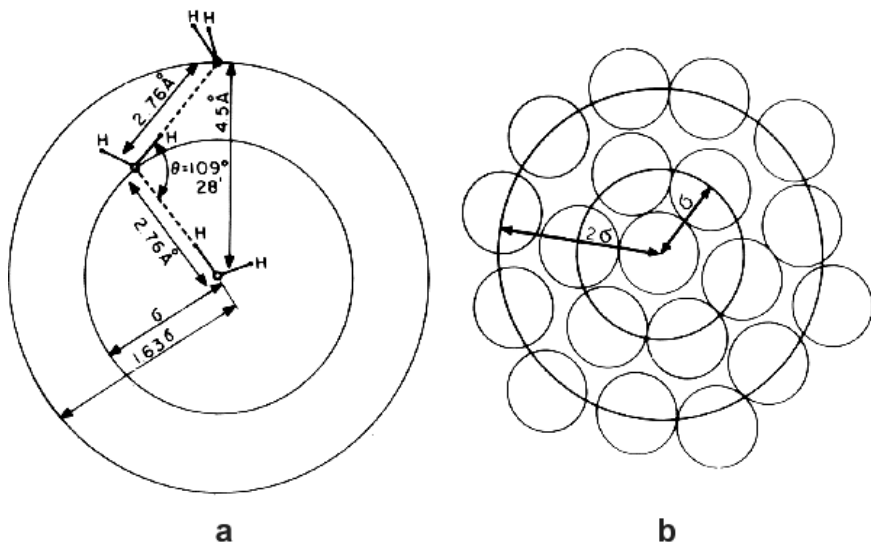


Fig. 1.29 The distribution of first and second neighbors in (a) water, and (b) a simple liquid.

Figure 1.29a shows the distances at which we can expect relatively higher densities around a central water molecule.

The full orientation-dependent pair correlation function cannot be obtained from experiments. Instead, only information on the *spatial* correlation function is obtainable. The spatial correlation function is defined as

$$g(\mathbf{R}_1, \mathbf{R}_2) = \frac{1}{(8\pi^2)^2} \iint d\Omega_1 d\Omega_2 g(\mathbf{R}_1, \Omega_1, \mathbf{R}_2, \Omega_2) \quad (1.4.5)$$

where the function $g(\mathbf{R}_1, \mathbf{R}_2)$ is a function of the scalar distance $R = |\mathbf{R}_2 - \mathbf{R}_1|$.

Water, as a hetero-atomic liquid, produces a diffraction pattern that reflects the combined effects of O-O, O-H, and H-H correlations. Thus, in principle, we have three distinct atom-atom pair correlation functions: $g_{OO}(R)$, $g_{OH}(R)$, and $g_{HH}(R)$. Earlier experimental data based on X-ray scattering could not be

resolved to obtain these three functions separately. Therefore, the only information obtained is a weighted average of these three functions. In all our future references to the experimental radial distribution function, we shall always refer to $g_{OO}(R)$, or simply $g(R)$. Recently, neutron scattering experiments have provided more detailed information on $g_{OO}(R)$, $g_{OH}(R)$, and $g_{HH}(R)$. We shall not need this additional information for the present book. For details, see Narten and Levy (1971), Soper (1996), Soper (2000), and Tromp *et al.* (1994).

Recently, Sorenson *et al.* (2000) reported new results for the oxygen-oxygen pair correlation function based on Advanced Light Source (ALS) X-ray scattering on pure liquid water. They found that their results at the second and third peak are nearly the same as the results reported by Narten and Levy (1971) and Soper *et al.* (1997). On the other hand, the location and the width of their results at the first peak differ considerably from the older results.

Figure 1.30 shows the *RDF* for water at 25°C obtained by X-ray (Narten and Levy, 1971) and by neutron scattering (Soper, 1997). As can be seen from the figure, the agreement between the two curves is quite good.³⁸

Figure 1.31 shows $g(R)$ for water and for argon, not as a function of R but as a function of the *reduced* distance $R^* = R/\sigma$. The reason we plot the *RDF* as a function of R/σ is to facilitate the comparison between the two functions. As we have seen, the first peak of $g(R)$ appears at the distance $R \approx \sigma$. Therefore, plotting $g(R^*)$ gives the first peaks of *RDF* of both argon and water at $R^* \approx 1$. First, we note that the curves for both argon and water are practically zero for $R^* \leq 1$. Second, the first peaks of the two curves are at about $R^* \approx 1$, and the

³⁸For more details, see Soper (1996), Soper (2000), Tromp *et al.* (1994), Soper and Philips (1986), Soper *et al.* (1997), Hura *et al.* (2003), and Sorenson *et al.* (2000).

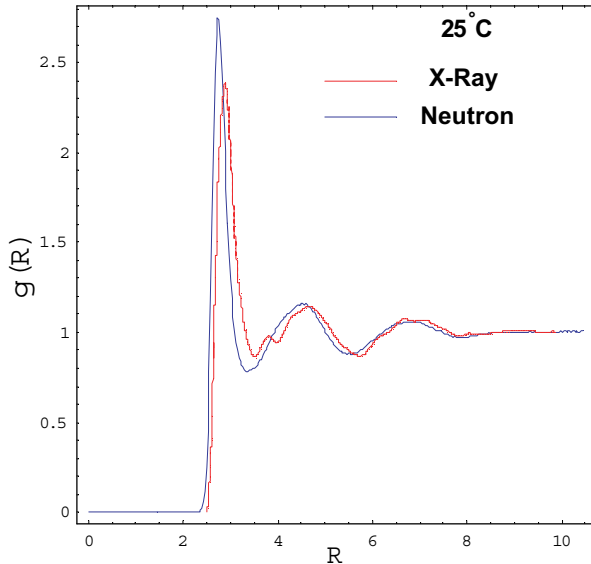


Fig. 1.30 The radial distribution function for water obtained from X-rays and neutron scattering [based on data from Narten and Levy (1971) and Soper (2000)].

two curves tend to unity for $R^* \geq 4$, i.e. beyond 4σ there is no more correlation.

The two curves in Fig. 1.31 differ in several aspects that are important for the understanding of liquid water. First, the curve of the water-*RDF* at about $R^* \approx 1$ is narrower, and its maximum value is lower than that of the argon-*RDF*. This is quite surprising. In general, one would have expected the first peak to be higher, the stronger the interaction. This is certainly true if we are in the gaseous phase, in which case the *RDF* is given by $g(R) \approx \exp[-\beta U(R)]$. Hence, the stronger the pair interaction, the higher the peak. However, in liquid water there is a unique mode of packing of the water molecules such that a strong binding energy is correlated with low local density (here, binding is simply the total interaction energy of a molecule with its surrounding molecules). We shall further discuss this peculiar correlation in Chapter 2.

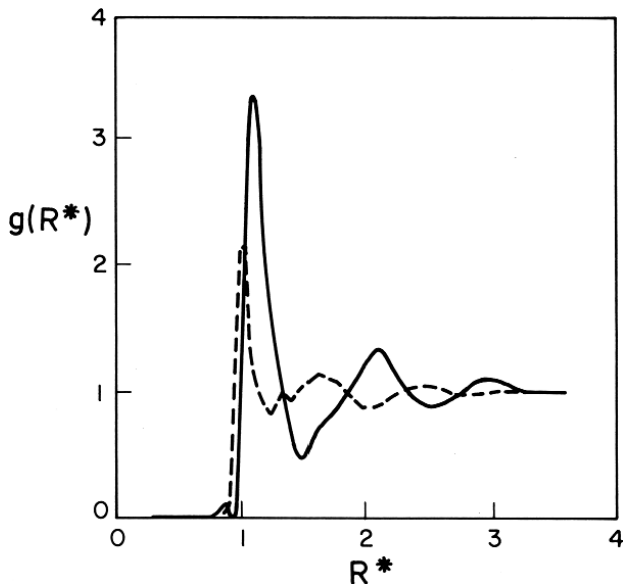


Fig. 1.31 Radial distribution function $g(R^*)$ for water (dashed line) at 4°C and 1 atm, and for argon (solid line) at 84.25 K and 0.71 atm , as a function of the reduced distance $R^* = R/\sigma$. (From Ben-Naim (1974) based on data for argon courtesy of N. S. Gingrich, and for water courtesy of A. H. Narten.)

Second, the area under the curve around the first peak is related to the differences in the local density or the coordination number in the two liquids. The coordination number is defined using the following procedure. We first choose a radius R_M ; then we determine the average number of particles contained within a sphere of radius R_M centered at any given particle in the system. Since $\rho g(R)4\pi R^2 dR$ is the average number of particles in a spherical shell of width dR and radius R , the average number of particles in the *entire sphere* of radius R_M is simply the sum of the average numbers of particles in all the spherical shells between $R = 0$ to $R = R_M$. This sum is the integral

$$CN(R_M) = \rho \int_0^{R_M} g(R)4\pi R^2 dR \quad (1.4.6)$$

Clearly, once we have $g(R)$, we can calculate $CN(R_M)$. In particular, we can define the first coordination number as the quantity $CN(R_M)$, for a choice of R_M , as the location of the first minimum of $g(R)$, following the first maximum. We shall denote the first coordination number as n_{CN} . The first coordination number for water at 4°C and 1 atm was estimated to be around 4.4. On the other hand, for liquid argon at 84.25°K and 0.7 bar the first coordination number is about 10. The latter value is typical of a close-packed liquid having a coordination number in the range of 10 to 12. On the other hand, the value of 4.4 for water is unusual for a liquid and is strongly reminiscent of the exact coordination number of the solid hexagonal ice I_h . It suggests that the “local structure” of water is very similar to the local structure of ice. No similar resemblance in local structure is observed in argon or in any other simple liquid. It is also of interest to note that the first coordination number of a simple liquid normally decreases with an increase in temperature. The opposite is true for liquid water. Since the location of the first minimum of the *RDF* changes with temperature, we have plotted in Fig. 1.32 the function $CN(R_M)$ for R_M between 3.3 Å to 3.7 Å. As can be seen from the figure if we choose $R_M \approx 3.3$ Å, we see that if we increase the temperature, the *CN* initially *increases*, but at higher temperatures it decreases with the increase in temperature. As the figure shows, the temperature dependence of the *CN* depends on the choice of R_M . Figure 1.33 shows for comparison the *RDF*, the coordination number as a function of R_M , and n_{CN} calculated for $R_M = 1.5$ and as a function of T for Lennard–Jones particles.³⁹

The third difference between the two *RDF* curves in Fig. 1.31 is the location of the second peak in the *RDF*. We have noted

³⁹These curves were calculated by Raymond Mountain using the molecular dynamics method.

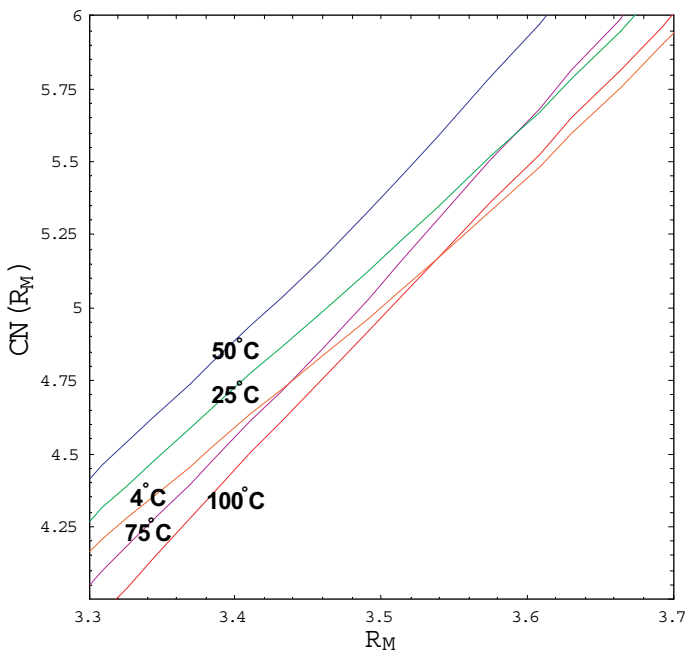


Fig. 1.32 Coordination number and its temperature dependence for water as a function of R_M [see Eq. (1.4.6)].

that for a simple liquid such as argon, a large correlation can be expected at about $R^* \approx 2$ (i.e. at a distance of $R = 2\sigma$). Indeed, we see that the *RDF* of argon has a peak at about $R^* \approx 2$. This is “normal” behavior, as we have explained before. In contrast, the *RDF* of water shows a second peak at an “abnormal” location at about $R^* \approx 1.6$, i.e. at a distance of $R = 1.6\sigma$. If we take $\sigma \approx 2.8 \text{ \AA}$ as the effective diameter of water, we have the second peak at $R = 4.5 \text{ \AA}$. What does this distance mean in terms of the packing mode of water molecules?

We recall that in the structure of ordinary ice (see Sec. 1.3) the O-O distance is 2.76 \AA . A simple calculation shows that the second-nearest neighbor distance between oxygens is $2 \times 2.76 \sin(\theta_T/2) = 4.5 \text{ \AA}$. This is the “ideal” O-O distance

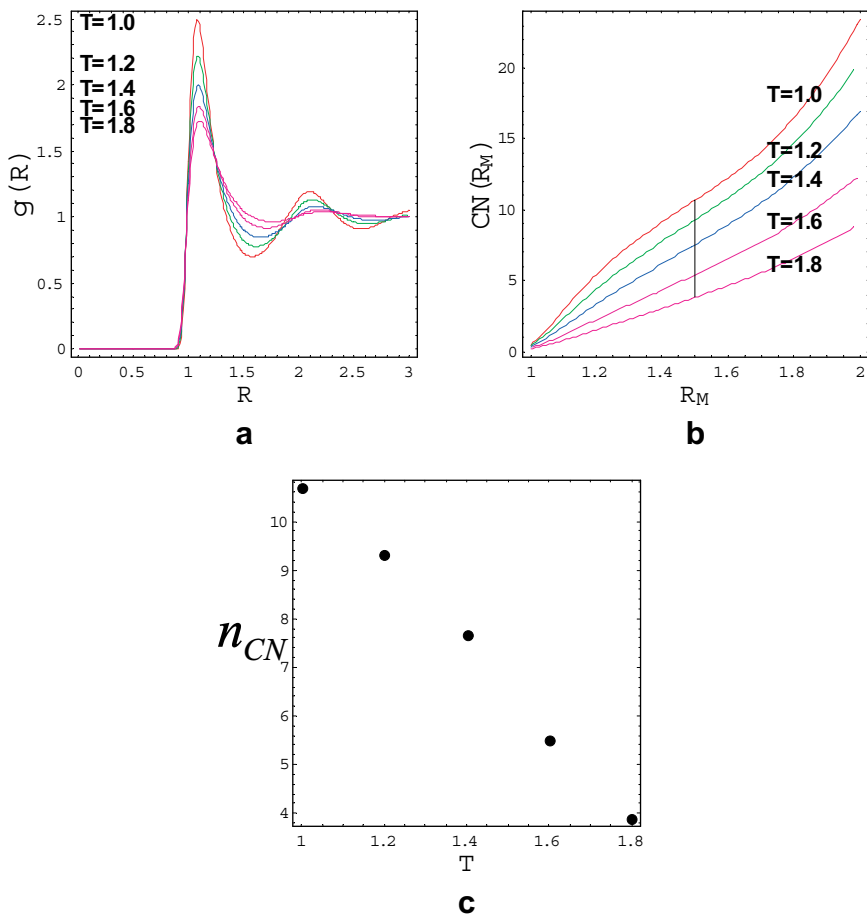


Fig. 1.33 (a) Radial distribution functions for Lennard–Jones particles at different temperatures, (b) coordination number as a function of R_M , and (c) coordination number as a function of T , for Lennard–Jones particles. All the calculations were performed by molecular dynamics in the T, P, N ensemble for LJ particles with $\sigma = 1$ and $\varepsilon/k_B = 1$. (The data was provided by Raymond Mountain.)

for second-nearest neighbor oxygens in ice. The fact that the second peak in the *RDF* of water is also found at 4.5 \AA means that the probability of finding second-nearest neighbors in liquid water is greatest at 4.5 \AA (see Fig. 1.29a). This, together

Table 1.8. First Coordination Numbers in Solid and Liquids^a

Substance	n_{CN} in solid	n_{CN} in liquid
Li	14	9.8
Na	14	9.3
K	14	8
Ar	12	10.2–10.9
Xe	12	8.5
Ga	7	7.8
Ge	4	8

^aFrom Samoilov (1957).

with the coordination number of water, is a strong indication that the local structure around a water molecule is very similar to the local structure around a water molecule in ice I_h .

Some authors consider the value of $g(R = 4.5 \text{ \AA})$ as a signature of the structure of water. This is basically correct.⁴⁰ However, in principle, a high peak at $R = 4.5 \text{ \AA}$ could also be a result of a large concentration of triplets of water molecules in the configuration as in Fig. 1.29a, not necessarily having the local structure of ice.

At this point in our discussion, it is clear that the *RDF* of water, $g(R)$, does reveal some qualitative information about the structure of liquid water. Thus far, we have not defined the

⁴⁰Note that some authors *define* the structure of a liquid in terms of the correlation functions. For instance, Fletcher (1970) writes: “From a statistical point of view, the structure of a liquid water is defined by a set of correlation functions; $g_n(R_1; R_2, \dots, R_n)$ which specify the probability that an atom can be found at the position R_1 , given that there are atoms at positions R_2, \dots, R_n .” In my opinion, this cannot serve as a definition of the structure of water. First, because these probabilities are defined for any liquid and there is no direct relationship between the values of these probabilities and the extent of *structure* as commonly understood. Second, one cannot use a whole *function* as a measure of structure. One needs a *number* that expresses the extent of structure which is typical of liquid water. We shall further discuss this topic in Chapter 2.

concept of water structure. In Chapter 2, we shall see that a single number that measures the degree of structure of water is needed for the understanding of both water and aqueous solutions.

These three features of the radial distribution function lead to the following conclusion. The basic geometry around a single molecule in water is, to a large extent, similar to that of ice. This is to say that, on average, each molecule has a coordination number of about four, and furthermore, there is a high probability that triplets of molecules will be found with nearly the same geometry as triplets of molecules at successive lattice points in ice. This conclusion pertains only to the *local* environment of a water molecule; no information whatsoever is furnished by $g(R)$ about the structure of the extended layer of molecules. In other words, if one were to sit at the center of a water molecule and observe the local geometry in a sphere of radius, say, 5 \AA , one would see most of the time a picture very similar to the one seen from an ice molecule, with frequent distortions caused by thermal agitation typical of the liquid state. These facts were recognized long ago by Bernal and Fowler and by Pauling. Beyond that radius (of about 5 \AA), the structure will not be recognized as that of ice.

Figure 1.34 shows the pair correlation function for H_2O and D_2O . It is clear that the two functions are almost identical. On the scale of this figure, the two curves cannot be distinguished. As we shall see in Chapter 2, this fact is consistent with the fact that the geometry of water and of the hydrogen bonds are nearly the same for the two liquids. However, the *structures* of the two liquids are not the same as could be erroneously deduced by comparing the *RDFs* of H_2O and D_2O .

The temperature dependence of $g(R)$ for water is shown in Fig. 1.35. There is a gradual shift in the location of the first peak from 2.84 \AA at 4°C to about 2.94 \AA at 100°C . A more characteristic feature is the rapid decay of the second peak, which

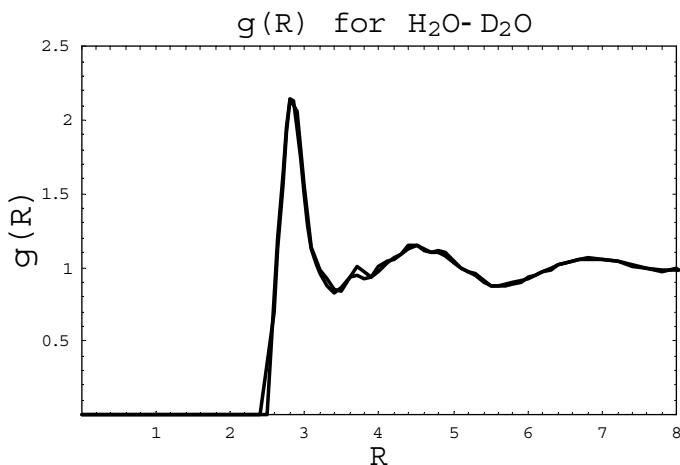


Fig. 1.34 The radial distribution function of water and heavy water at 4°C.

is almost unrecognizable at 100°C. Narten and Levy (1971) also reported the *RDF* at 150°C and 200°C. It is not clear at which pressures these results were obtained. In Fig. 1.36, we compare the *RDF* at 100°C and 150°C. As can be seen, there is almost no change in the curve around the first peak while beyond the first peak there is not much of a structure at either temperature.

1.5. The Kirkwood–Buff Integral

Recently, a new way of studying, analyzing, and interpreting liquid mixtures has been suggested.⁴¹ The traditional approach to mixtures is based on the study of the excess thermodynamic quantities such as excess free energy, excess entropy, and enthalpy volume.⁴² These quantities convey macroscopic

⁴¹Ben-Naim (2006, 2008d).

⁴²Prigogine (1957), Van Ness and Abbott (1982), and Rowlinson and Swinton (1982).

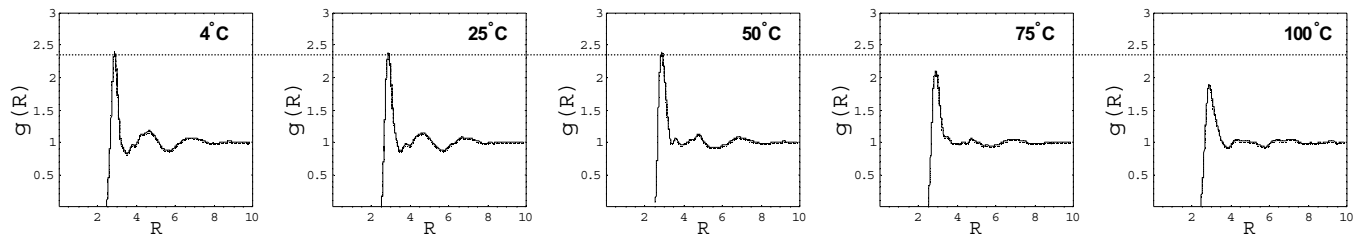


Fig. 1.35 The temperature dependence of $g(R)$ of water [based on data from Narten and Levy (1971)].

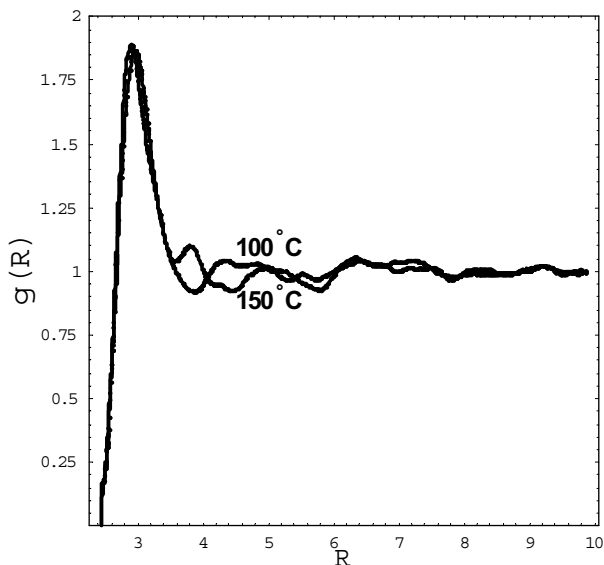


Fig. 1.36 The radial distribution function for water at 100°C and 150°C [based on data from Narten and Levy (1971)].

information and were thus referred to as *global* properties of the mixtures. The new approach is based on the so-called Kirkwood–Buff integrals (*KBI*). These quantities probe into the immediate surroundings of the molecules, and therefore are referred to as the *local* properties of the mixtures. For mixtures, the *KBIs* provide rich and interesting information on the local densities, local composition, and preferential solvation around a single molecule in the mixtures. In addition, the solvation thermodynamic quantities provide information on the strength of the interaction of a molecule with its environment, the effect of a molecule on the “structure” of the solvent, and so on (see Sec. 1.6).

Nowadays, it is common to refer to the quantities

$$G_{\alpha\beta} = \int_V [g_{\alpha\beta}(R) - 1] dR \quad (1.5.1)$$

as the Kirkwood–Buff integrals. They were used in the original “Kirkwood–Buff theory of solutions” published in 1951.⁴³ However, the same integrals were introduced much earlier by Ornstein and Zernike⁴⁴ in connection with the fluctuation in the number of particles in an open system of *one* component. In this section, we report on some values of the *KBIs* for one-component systems.

The Kirkwood–Buff integral (*KBIs*) for a one-component system is defined by

$$G_O = \int_V [g_O(R) - 1] d\mathbf{R} \quad (1.5.2)$$

where $g_O(R)$ is the pair correlation function, or the radial distribution function defined in an open system (or in the grand canonical ensemble); the integration is extended over the entire macroscopic volume of the system V . Note that R in $g(R)$ is the intermolecular distance, whereas $d\mathbf{R}$ is an element of volume $dx dy dz$.

The *KBI* is related to two macroscopic quantities by the equations⁴⁵

$$\frac{\langle N^2 \rangle - \langle N \rangle^2}{\langle N \rangle} - 1 = \rho G_O = k_B T \rho \kappa_T - 1 \quad (1.5.3)$$

where k_B is the Boltzmann constant, T is the absolute temperature, ρ is the average number density N/V in the system, and κ_T is the isothermal compressibility of the system.

On the left-hand side of (1.5.3), we have the fluctuations in the number of particles in the open system. On the right-hand side, we have a connection with macroscopic measurable

⁴³Kirkwood and Buff (1951).

⁴⁴Ornstein and Zernike (1914).

⁴⁵Hill (1956), Münster (1969), and Hansen and McDonald (2006).

quantities. This side of the equation is known as the compressibility equation.⁴⁵

It should be emphasized that Eq. (1.5.3) is valid only when G_O is defined as in (1.5.2) in an *open* system (hence the subscript O). Failing to recognize this fact has been a notorious pitfall. To see this we first write the *KBI*, defined in the same way as in (1.5.2), but in a *closed* system (hence the subscript C).

$$G_C = \int_V [g_C(R) - 1] d\mathbf{R} \quad (1.5.4)$$

The two quantities G_O and G_C look deceptively similar (and identical if we remove the subscripts C and O) but, in fact, they are quite different. The difference between the two can be demonstrated even for an ideal gas (see Appendix C). For any liquid, and at any density, the closure condition, i.e. the fixed number of particles in the system, imposes the normalization condition on G_C :

$$G_C = \int_V [g_C(R) - 1] d\mathbf{R} = -1/\rho \quad (1.5.5)$$

Clearly, this condition arises from the fact that the total number of particles N in the system is conserved, i.e.

$$N = \rho \int_V d\mathbf{R} = \rho \int_V g_C(R) d\mathbf{R} + 1 \quad (1.5.6)$$

On the right-hand side of (1.5.6), the counting of the total number of particles is done in two steps; first, count the number of particles around a selected particle, then add the selected particle to get N . As was pointed out by Münster (1969), if one uses the same notation for $g_C(R)$ and $g_O(R)$, and substitute the integral in (1.5.6) into the compressibility equation (1.5.3), one gets the *absurd* result $\kappa_T = 0$. Clearly, this result can be avoided

by using different notations for the pair correlation functions in the closed and open systems.

We know from both experimental data on the pair correlation functions and from theoretical calculation that the pair correlation function is significantly larger than unity only in a small region about the center of a given molecule. In other words, there exists a correlation length R_{CORR} such that for $R \geq R_{CORR}$, $g(R)$ is practically unity. This fact allows us to deduce *local* information from G_O (but not from G_C). To see this, it is convenient to rewrite the KBI as

$$\int_V [g(R) - 1] d\mathbf{R} = \int_{V_{CORR}} + \int_{V - V_{CORR}} \quad (1.5.7)$$

where $V_{CORR} = 4\pi R_{CORR}^3/3$ is the correlation volume, which is essentially a *microscopic* volume, and $V - V_{CORR}$ is the *macroscopic* volume V of the system minus V_{CORR} . It is well known that the pair correlation function in the region $V - V_{CORR}$ is different in open and closed systems, i.e.

$$g_O(R \geq R_{CORR}) \cong 1 \quad (1.5.8)$$

$$g_C(R \geq R_{CORR}) \cong 1 - \frac{k_B T \rho \kappa T}{N} \quad (1.5.9)$$

From (1.5.8) and (1.5.7) it follows that the second integral on the right-hand side of (1.5.7) can be neglected in G_O , but not in G_C . Hence, we have

$$\begin{aligned} G_O &= \int_V [g_O(R) - 1] d\mathbf{R} \\ &= \int_0^\infty [g_O(R) - 1] 4\pi R^2 dR \\ &\approx \int_0^{R_{CORR}} [g_O(R) - 1] 4\pi R^2 dR \end{aligned} \quad (1.5.10)$$

$$G_C = \int_0^{R_{CORR}} [g_C(R) - 1] 4\pi R^2 dR - \frac{k_B T \rho \kappa T}{\rho'} \quad (1.5.11)$$

where $\rho = N/V$ and $\rho' = N/(V - V_{CORR})$. Thus, because of (1.5.10), G_O itself provides *local* information around a molecule. Furthermore, since in the correlation region ($R \leq R_{CORR}$) the values of $g_C(R)$ and $g_O(R)$ are nearly the same, the same local information is also contained in the integral of (1.5.11). However, in this case this integral is not equal to G_C . Therefore, we cannot identify the local information contained in G_O with G_C . Another way of viewing the different behaviors of open and closed systems is shown schematically in Fig. 1.37. In a closed system with *fixed* density $\rho = N/V$, placing one particle at the center of a sphere of radius R_{CORR} will change the density in the region $R_{CORR} \leq R \leq R_M$, where R_M is the radius of the macroscopic system, from $\rho = N/V$ to $\rho^* = \rho(1 - \frac{k_B T \rho k_T}{N})$. The same process in an open system does not change the density ρ .

Thus, for an open system one can replace the integral over the entire region V by an integral over the correlation region. This makes the *KBI*, G_O , useful for studying local quantities, such as local density, local composition, and local preferential solvation (Ben-Naim, 2006). The same is not true for G_C , for

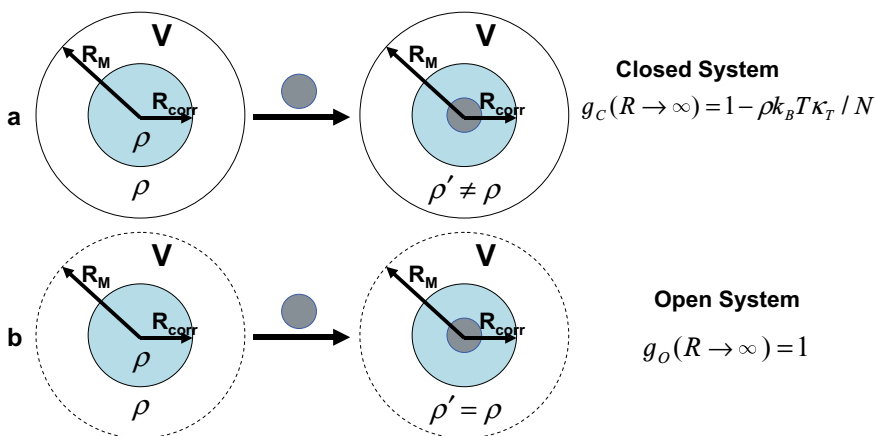


Fig. 1.37 The effect of placing a particle (dark disk) at the center of the correlation sphere (blue disk) in (a) closed, and (b) open systems.

which the second integral on the right-hand side of (1.5.7) is finite.

The *local* meaning of the KBI (G_O , but not G_C) is the following: $\rho 4\pi R^2 dR$ is the average number of particles in a spherical shell of radius R and width dR . $\rho g_O(R) 4\pi R^2 dR$ is the average number of particles in the same spherical shell, but in the center of which a particle is placed. Therefore, $\int_0^{R_{CORR}} \rho [g_O(R) - 1] 4\pi R^2 dR$ is the *change* in the average number of particles in the sphere of radius R_{CORR} , caused by placing a particle at the center of the sphere. Because of the property (1.5.8) in the open system, one can replace the upper limit R_{CORR} by infinity to obtain the same interpretation for the KBI (G_O but not G_C).

Another useful relation between the KBI and the partial molar volume at a fixed position is (Ben-Naim, 2006)

$$G_O = -V^* \quad (1.5.12)$$

Note that the molar volume V_M is the change in the volume of the system caused by adding one mole (or one molecule, depending on the context) of particles to the system at constant T and P . The quantity V^* is the change in the volume of the system caused by placing a particle at a *fixed position* in the system, keeping T and P constant. The relation between the two volumes (per particle) is

$$V_M = V^* + k_B T \kappa_T \quad (1.5.13)$$

From (1.5.12) it follows that

$$\rho G_O = \Delta N(R_{CORR}) = -\rho V^* \quad (1.5.14)$$

Thus, the change in the average number of particles in the correlation volume $\Delta N(R_{CORR})$ caused by placing a particle at the center of the correlation volume is equal to minus the

average number of particles occupying the volume V^* in the liquid having the density ρ .

It is sometimes convenient to reinterpret the *KBI* as follows (we drop the subscript O in the rest of this section since we shall always refer to G_O and not to G_C):

$$\begin{aligned}
 G &= \int_V [g(R) - 1] d\mathbf{R} \\
 &= \int_{V^{EX}} + \int_{V - V^{EX}} \\
 &= -V^{EX} + \int_{V - V^{EX}} [g(R) - 1] d\mathbf{R} \\
 &= -V^{EX} + L
 \end{aligned} \tag{1.5.15}$$

where V^{EX} is the excluded volume. This is defined as the region around the center of the particle for which $g(R) \cong 0$; hence, the integration over this region produces the negative quantity $-V^{EX}$. For spherical particles with hard-core diameter σ , this volume is simply

$$V^{EX} = \frac{4\pi\sigma^3}{3} \tag{1.5.16}$$

Thus, in general, G has two contributions: $-V^{EX}$, which is always negative, and L , which may be either positive or negative depending on the strength of the correlation function in the region $V_{CORR} - V^{EX}$.

We now present a few examples of the *KBIs*.

1.5.1. *Ideal gas*

Ideal gas behavior can be realized by either systems of hypothetical, *strictly-non-interacting* particles, or by real particles but at the limit of low densities $\rho \rightarrow 0$. Both of these give the same

equation of state

$$P = \rho k_B T \quad (1.5.17)$$

However, the two systems produce different *KBIs*. For the hypothetical ideal gas, all intermolecular interactions are zero, and hence, the pair correlation function is unity, and therefore

$$G(\text{hypothetical i.g.}) = 0. \quad (1.5.18)$$

Note that this equality is not true for the *KBI* defined in a closed system (see Appendix C).

For the *real* ideal gas, i.e. a system of interacting particles at $\rho \rightarrow 0$, we have the limiting value of the *KBI*:

$$G(\text{real i.g.}) = \lim_{\rho \rightarrow 0} G = \int_V \{\exp[-\beta U(R)] - 1\} d\mathbf{R} \quad (1.5.19)$$

This limit follows from the well-known expression for the pair correlation function at $\rho \rightarrow 0$, namely⁴⁶

$$g(R) \xrightarrow{\rho \rightarrow 0} \exp[-\beta U(R)] \quad (1.5.20)$$

where $U(R)$ is the pair potential.

The simplest interacting particles are hard spheres for which

$$U_{HS}(R) = \begin{cases} \infty & \text{for } R \leq \sigma \\ 0 & \text{for } R > \sigma \end{cases} \quad (1.5.21)$$

Hence,

$$G(\text{hard spheres}, \rho \rightarrow 0) = -\frac{4\pi\sigma^3}{3} \quad (1.5.22)$$

This is simply the excluded volume for the hard-sphere particles.

⁴⁶Hill (1956), Münster (1969), and Ben-Naim (2006).

For a *real* ideal gas, we can write

$$G(\text{real i.g.}) = \frac{-4\pi\sigma^3}{3} + \int_{V-V_{EX}} \{\exp[-\beta U(R) - 1]\} d\mathbf{R} \quad (1.5.23)$$

where σ is the *effective* hard-core diameter. For Lennard–Jones (*LJ*) particles, the effective hard-core diameter can be chosen as the parameter σ in the Lennard–Jones potential (see Sec. 1.2 and Table 1.3). For such a system, G consists of two terms: one negative due to the excluded volume and one positive due to the positive correlation (i.e. $g(R) \geq 1$ in the region $R \geq \sigma$). The two corresponding regions of the integrand in (1.5.19) are shown in Fig. 1.38. Here, we have a clear-cut separation between the positive and negative contributions to G .⁴⁷

1.5.2. Inert gases represented as Lennard–Jones particles

Lennard–Jones (*LJ*) particles are defined through the pair potential

$$U_{LJ}(R) = 4\epsilon \left[\left(\frac{\sigma}{R}\right)^{12} - \left(\frac{\sigma}{R}\right)^6 \right] \quad (1.5.24)$$

Figure 1.39 shows the functions $g(R)$ and $G(R_M)$ for the Lennard–Jones parameters corresponding to neon, argon, krypton, and xenon. All the plots are based on equations (1.5.24) and calculated for $T = 273$ K

$$G(R_M) = \int_0^{R_M} [g(R) - 1] 4\pi R^2 dR \quad (1.5.25)$$

⁴⁷We neglect the region between σ and $\sqrt[6]{2}\sigma$, where the potential is repulsive but $g(R)$ is smaller than unity.

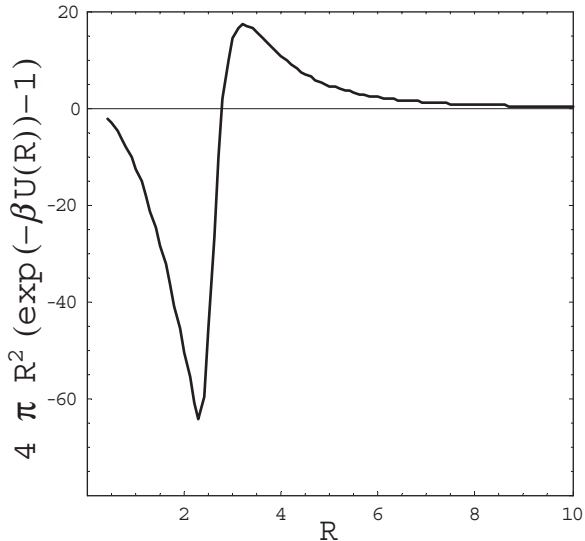


Fig. 1.38 The integrand $\{\exp[-\beta U(R)] - 1\}4\pi R^2$ as a function of R for LJ particles with parameters $\sigma = 2.78 \text{ \AA}$, $\varepsilon/k_B = 34.9 \text{ K}$ and at $T = 273 \text{ K}$. The negative and the positive regions contribute negative and positive values to the integral G in (1.5.19), respectively.

where

$$g(R) = \exp[-\beta U(R)] \quad (1.5.26)$$

with parameters given in Table 1.3. As can be seen from Fig. 1.39, for neon at very low densities, the excluded volume term V^{EX} in (1.5.15) is the dominant contribution to G , making the value of G negative. In all other cases, the values of G are positive, indicating that the attractive part of the potential dominates in (1.5.15) and the resulting values of G are all positive.

1.5.3. Water, methanol, and ethanol

Figure 1.40 shows the KBI for a series of linear alcohols having the formula $\text{CH}_3(\text{CH}_2)_{n-1}\text{OH}$ as a function of the number of carbon atoms. It is seen that the values are all negative and

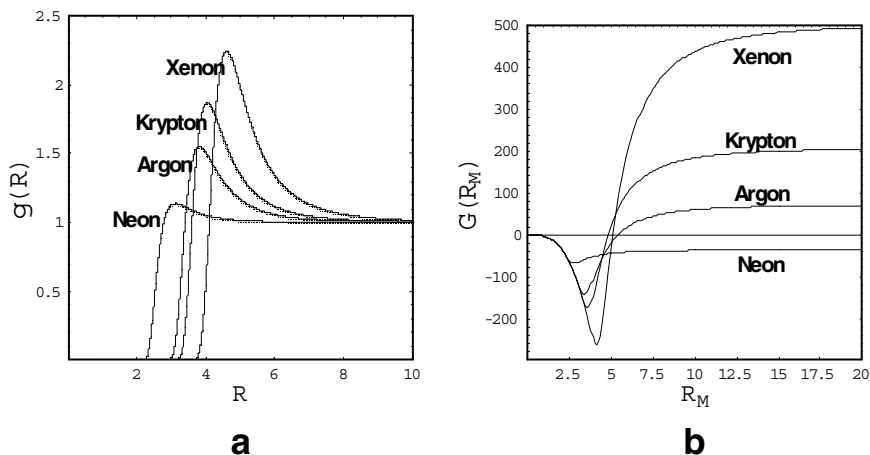


Fig. 1.39 Values of $g(R)$ and $G(R_M)$ for inert gases at low densities ($\rho \rightarrow 0$) with parameters given in Table 1.3 and $T = 273$ K.

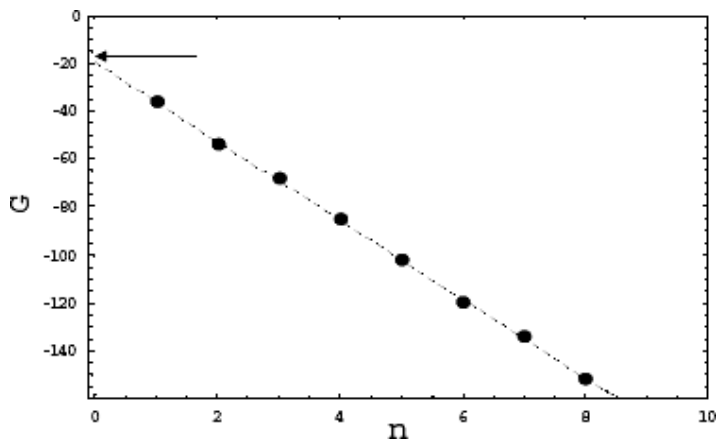


Fig. 1.40 Values of G for pure linear alcohols at 1 atm and 25°C . The extrapolated value at $n = 0$ is indicated by the arrow.

decrease with n . Clearly, the larger the chain, the larger the contribution from the hard-core repulsion, and hence, the more negative the value of the KBI . If we extrapolate from these values to $n = 0$, we get the value of G for the *hypothetical* alcohol

with no carbon atoms. Interestingly, the value of the *KBI* for water almost coincides with the extrapolated value from the series of alcohols. This finding is quite puzzling for the following reasons. As can be seen from Eq. (1.5.3), the *KBI* is determined by both the molar volume and the compressibility of water. These two properties show anomalous behavior as a function of temperature, yet the combination of the two produces a quantity that seems to behave “normally.”

Figure 1.41 shows the values of *G* for water as a function of temperature at 1 atm. From what we know about water, we would have expected for a small molecule such as water, with an effective diameter similar to that of neon and with such strong interactions (hydrogen bonding), that the positive contribution to the *KBI* would dominate the value of *G*. Yet the values of the *KBI* of liquid water are all negative over the entire range of temperatures. On the other hand, the *KBI* for low density steam has large and positive values (see Fig. 1.41c). The reason is that in the gaseous phase at low density, the pair interaction determines the pair correlation function [Eq. (1.5.26)]. Hence, strong interactions (hydrogen bonding) should contribute large positive values to the *KBI*. In the liquid state, the pair correlation function is determined not only by the pair interactions but also by higher order, non-additive potentials. The net effect of these interactions is to produce a relatively narrow first peak of the pair correlation function of water. This is equivalent to small coordination numbers. Hence, in this case the effect of the strong attractive forces is reduced and the value of *G* becomes negative.

Note that the values of *G* for D_2O are systematically lower than the corresponding values of H_2O . This curve goes through a maximum value at about $6^\circ C$ (not corresponding to either the minimum of the volume or the compressibility of D_2O).

Since H_2O and D_2O have almost the same effective diameters, one cannot explain the larger negative values of *G* of D_2O

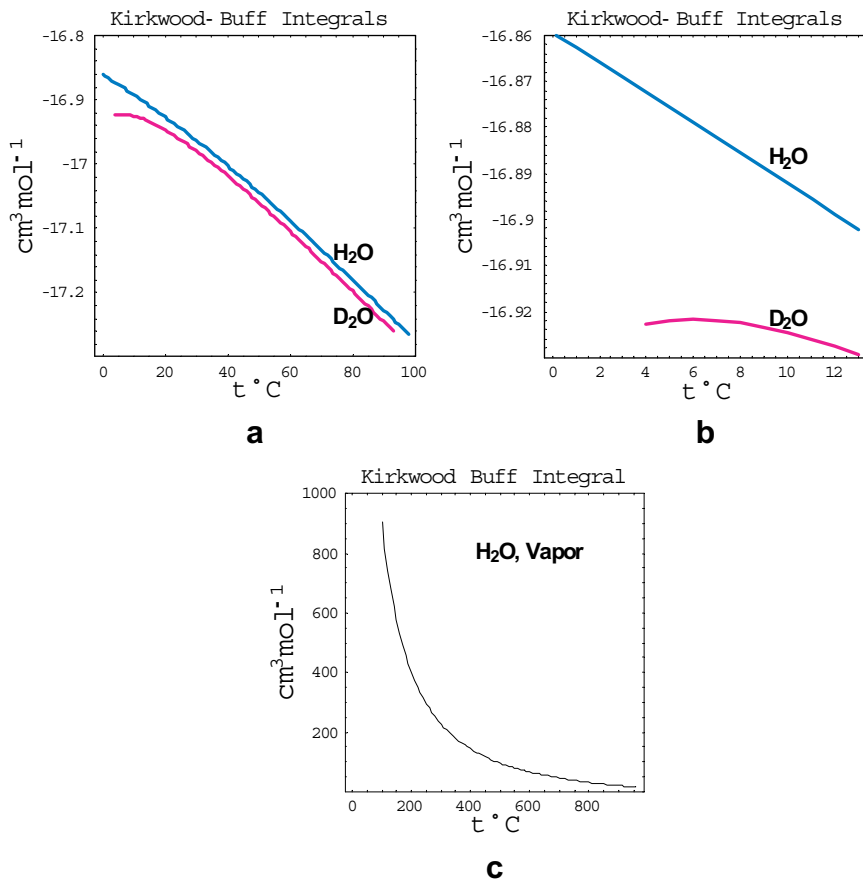


Fig. 1.41 (a) Values of G for H_2O and D_2O as a function of temperature at 1 atm, (b) details at low temperatures, and (c) the KBI for water vapor.

due to a larger excluded volume. Hence, Eq. (1.5.15) is of no help in this regard. On the other hand, looking at the compressibility equation, we notice that the term $k_B T \kappa_T$ is much smaller than the molar volume V_M . We can interpret the difference in the $KBIs$ of H_2O and D_2O in terms of the molar volumes. The molar volumes in turn may be interpreted in terms of the “relative degree of structure” of the two liquids. The strength of

the hydrogen-bond (*HB*) energy of D_2O is known to be larger than that of H_2O . Therefore, it is reasonable to expect that, on average, more molecules are being engaged in hydrogen bonding in D_2O . This leads to a larger concentration of the open structure component, and hence, to a larger negative *KBI*. We shall further discuss the structures of H_2O and D_2O in Chapter 2.

The pressure dependence of the *KBI* for H_2O and D_2O at $25^\circ C$ is shown in Fig. 1.42. The two curves are almost linear and almost parallel to each other. Again, we see that D_2O has the larger (negative) values of the *KBI* in the entire range of pressures.

Figure 1.43 shows the *KBI* for some hydrocarbons and for methanol and ethanol as a function of temperature at 1 atm. Since in each group the overall attractive part of the intermolecular interactions have similar magnitude, the relative difference in the *KBI*s is expected to depend on the size of the molecules.

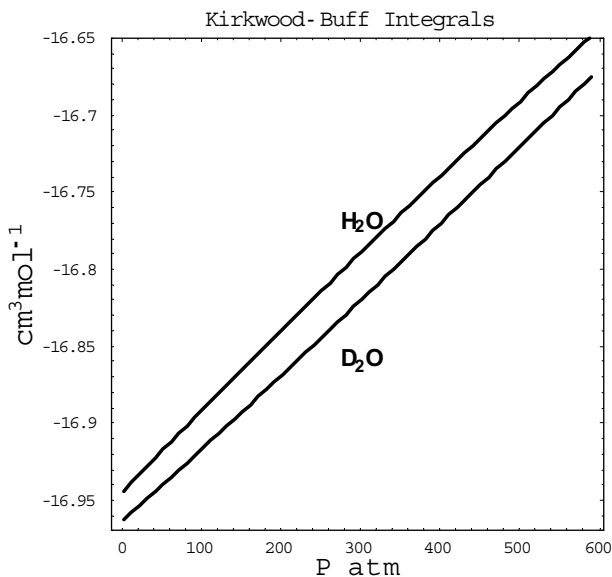


Fig. 1.42 The pressure dependence of *G* for H_2O and D_2O at $25^\circ C$.

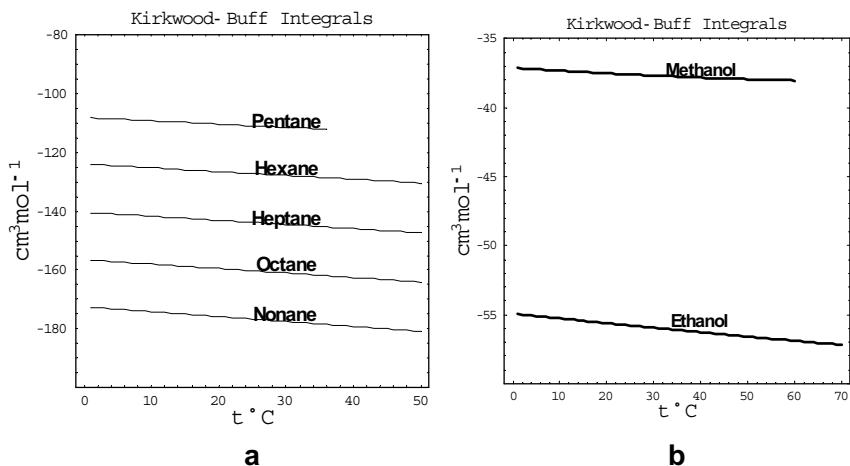


Fig. 1.43 Values of G for (a) some linear hydrocarbons, and (b) methanol and ethanol as a function of temperature at 1 atm.

In this figure, all the *KBIs* are negative and the temperature dependence is also negative.

1.6. Solvation of Water in Water

Another set of quantities which also convey information of *local* character are the solvation thermodynamic quantities.

We shall discuss at length solvation quantities in Chapter 3. Here, we present some values of the thermodynamics of solvation of water in pure water. It should be noted that in the traditional approach to solvation, only solvation of one component in very dilute solution in a solvent can be defined and measured. In the definition used here, the concept of solvation can be applied to any molecule in any liquid at any concentration.⁴⁸

We define the solvation process as the transfer of a molecule from a fixed position in an ideal gas phase to a fixed position

⁴⁸For details, see Ben-Naim (2006).

in the liquid. The statistical mechanical expression for the solvation Gibbs energy follows directly from the definition of the solvation process. We define the pseudo-chemical potential in the liquid by

$$\mu_w^{*l} = -k_B T \ln \frac{\Delta^l(T, P, N + 1, \mathbf{R}_0)}{\Delta^l(T, P, N)} \quad (1.6.1)$$

where $\Delta^l(T, P, N)$ is the T, P, N partition function (PF) of pure water at T, P, N . $\Delta^l(T, P, N + 1, \mathbf{R}_0)$ is the PF for a system at the same T and P but with an additional water molecule placed at some fixed position in the liquid.

Likewise, we define the pseudo-chemical potential of water in an ideal gas phase as

$$\mu_w^{*ig} = -k_B T \ln \frac{\Delta^{ig}(T, P, N + 1, \mathbf{R}_0)}{\Delta^{ig}(T, P, N)} \quad (1.6.2)$$

where Δ^{ig} are the corresponding PF s, in the ideal gas phase.

The solvation Gibbs energy is now defined by

$$\Delta G_w^* = \mu_w^{*l} - \mu_w^{*ig} \quad (1.6.3)$$

It is easy to show that if we assume that the internal degrees of freedom of the solvated molecules are not affected by the solvation process, then we have the expression⁴⁹

$$\Delta G_w^* = -k_B T \ln \langle \exp[-\beta B_w] \rangle_0 \quad (1.6.4)$$

where B_w is the total interaction energy of the added molecule with all the particles in the liquid, and the average $\langle \cdot \rangle_0$ is over all the configurations of the N molecules (excluding the added molecule) and all possible volumes of the system at given T, P, N .

⁴⁹See Ben-Naim (2006).

Equation (1.6.4) is important for the theoretical interpretation of the solvation quantities (see Chapters 2 and 3). Here, we are interested in the method of calculating the quantity ΔG_w^* from experimental data. This is obtained as follows. We write the chemical potentials of w in the liquid and in the gaseous phases at equilibrium

$$\mu_w^l = \mu_w^{*l} + k_B T \ln \rho_w^l = \mu_w^g = \mu_w^{*g} + k_B T \ln \rho_w^g \quad (1.6.5)$$

From (1.6.5) it follows that

$$\mu_w^{*l} - \mu_w^{*g} = k_B T \ln (\rho_w^g / \rho_w^l)_{eq} \quad (1.6.6)$$

Note that, in general, this quantity is different from the quantity defined in (1.6.3). Equation (1.6.6) is more general than (1.6.3) since it applies to any phase g , not necessarily an ideal gas phase. If we can assume that the vapor in equilibrium with the liquid is an ideal gas, then (1.6.6) becomes the solvation Gibbs energy as defined in (1.6.3). In the more general case, (1.6.6) is the *difference* in the solvation Gibbs energies in the two phases, i.e.

$$\begin{aligned} \Delta G_w^{*l} - \Delta G_w^{*g} &= \mu_w^{*l} - \mu_w^{*g} - (\mu_w^{*g} - \mu_w^{*g}) \\ &= \mu_w^{*l} - \mu_w^{*g} \end{aligned} \quad (1.6.7)$$

Figure 1.44 shows the values of $\Delta G_s^{*l} - \Delta G_s^{*g}$ (s can be either H_2O or D_2O) for water and heavy water in the entire range of the liquid state. Note that the values for D_2O are systematically lower than those for H_2O . As we increase the temperature along the liquid-vapor equilibrium line, the densities of the two phases become closer and closer. The values of $\Delta G_w^{*l} - \Delta G_w^{*g}$ become smaller and smaller, and at the critical point they should approach zero.

In the range of temperatures between 0°C to 100°C , we can assume that the vapor above the liquid is nearly ideal

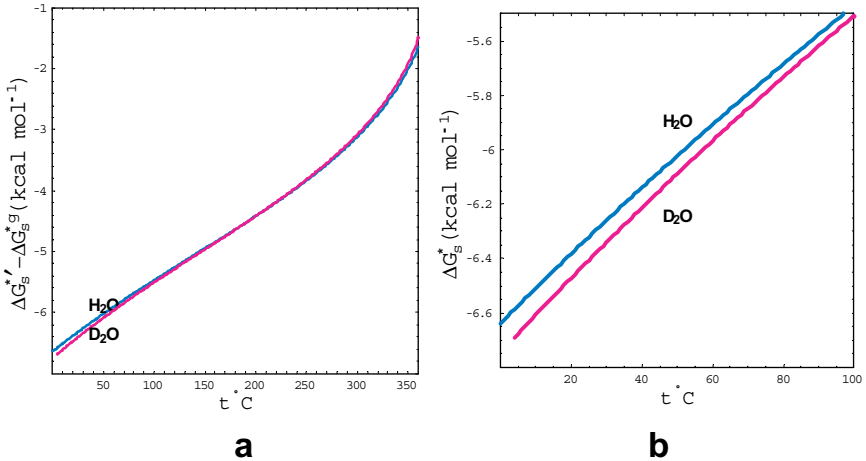


Fig. 1.44 (a) The difference in the solvation Gibbs energy between two phases for H₂O and D₂O as a function of temperature along the vapor-liquid equilibrium line. (b) Solvation Gibbs energies at lower temperatures.

gas. In this case, the values of $\Delta G_w^{*l} - \Delta G_w^{*g}$ in Fig. 1.44b are approximately equal to the solvation Gibbs energies in the liquid phase.

If the density of the vapor can be assumed to be an ideal gas, then

$$\frac{P_s}{k_B T} = \rho_s^{*ig} \quad (1.6.8)$$

where P_s is the vapor pressure of the pure liquid s . In this case, the solvation Gibbs energy of s in pure liquid s can be calculated from:

$$\Delta G_s^{*l} = k_B T \ln \left(\frac{\rho_s^{ig}}{\rho_s^l} \right)_{eq} = k_B T \ln \left(\frac{\rho_s}{k_B T \rho_s^l} \right)_{eq} \quad (1.6.9)$$

When evaluating other thermodynamic quantities of solvation from data along the equilibrium line, care must be exercised to distinguish between derivatives at *constant pressure* and

derivatives *along the equilibrium line*. The connection between the two is

$$\left(\frac{d\Delta G_s^{*l}}{dT}\right)_{eq} = \left(\frac{\partial\Delta G_s^{*l}}{\partial T}\right)_P + \left(\frac{\partial\Delta G_s^{*l}}{\partial P}\right)_T \left(\frac{dP}{dT}\right)_{eq} \quad (1.6.10)$$

Here, we used straight derivatives to indicate differentiation along the equilibrium line. The two derivatives of ΔG_s^* on the right-hand side of (1.6.10) are identified as the solvation entropy and the solvation volume, respectively, i.e.

$$\left(\frac{d\Delta G_s^{*l}}{dT}\right)_{eq} = -\Delta S_s^{*l} + \Delta V_s^{*l} \left(\frac{dP}{dT}\right)_{eq} \quad (1.6.11)$$

Usually, data are available to evaluate both of the straight derivatives in Eq. (1.6.11). This is not sufficient, however, to compute both ΔS_s^{*l} and ΔV_s^{*l} . Fortunately, ΔV_s^{*l} may be obtained directly from data on molar volume and compressibility of the pure liquid.

The relationship between the molar volume and the pseudo molar volume is⁵⁰

$$\bar{V}_s^l = \left(\frac{\partial\mu_s^l}{\partial P}\right)_T = V_s^{*l} + k_B T \kappa_T^l \quad (1.6.12)$$

where κ_T^l is the isothermal compressibility of the pure s .

Fortunately, the term $k_B T \kappa_T^l$ in liquids is small compared with the values of V_s^{*l} . Furthermore, the term $\Delta V_s^{*l} \left(\frac{dP}{dT}\right)_{eq}$ in (1.6.11) is also small compared with ΔS_s^{*l} . These facts may be used to calculate approximate values of both ΔV_s^{*l} and ΔS_s^{*l} from data on the densities of s at equilibrium between the gas and the liquid phases.

⁵⁰The pseudo molar volume is the pressure derivative of the pseudo-chemical potential (Ben-Naim, 2006).

The solvation volume is defined as

$$\Delta V_s^{*l} = V_s^{*l} - V_s^{*g}. \quad (1.6.13)$$

With ΔV_s^{*l} and $(\partial P/\partial T)_{eq}$, we can solve (1.6.11) for ΔS_s^{*l} , and from ΔS_s^{*l} we also get

$$\Delta H_s^{*l} = \Delta G_s^{*l} + T\Delta S_s^{*l} \quad (1.6.14)$$

$$\Delta E_s^{*l} = \Delta H_s^{*l} - P\Delta V_s^{*l} \quad (1.6.15)$$

and the heat capacity of solvation

$$\Delta C_{P,s}^{*l} = \left(\frac{\partial \Delta H_s^{*l}}{\partial T} \right)_P$$

Figure 1.45 shows the values of ΔG_s^{*l} , ΔS_s^{*l} , and ΔH_s^{*l} . Figure 1.46 shows values of ΔV_s^{*l} and $\Delta C_{P,s}^{*l}$. In Figs. 1.47 and 1.48 we present some values for the solvation quantities for methanol and ethanol.

1.7. The Importance of Water in Biological Systems

It is hardly necessary to emphasize the importance of water to life. Water in the blood not only runs through our bodies, but also runs our bodies. We need to constantly supply our body with water in order to keep it going. Water, as a solvent, helps distribute various chemicals needed in the different parts of the body, and at the same time it helps to discharge other waste chemicals that are not needed, or those that are even harmful. But water does much more than merely transport chemicals around the body. It affects in specific ways a multitude of biochemical processes taking place in each of our cells. It has long been speculated that life as we know it on this planet could not have started without water. Although this is merely speculation, it is a reasonable one. Strictly speaking of course, we

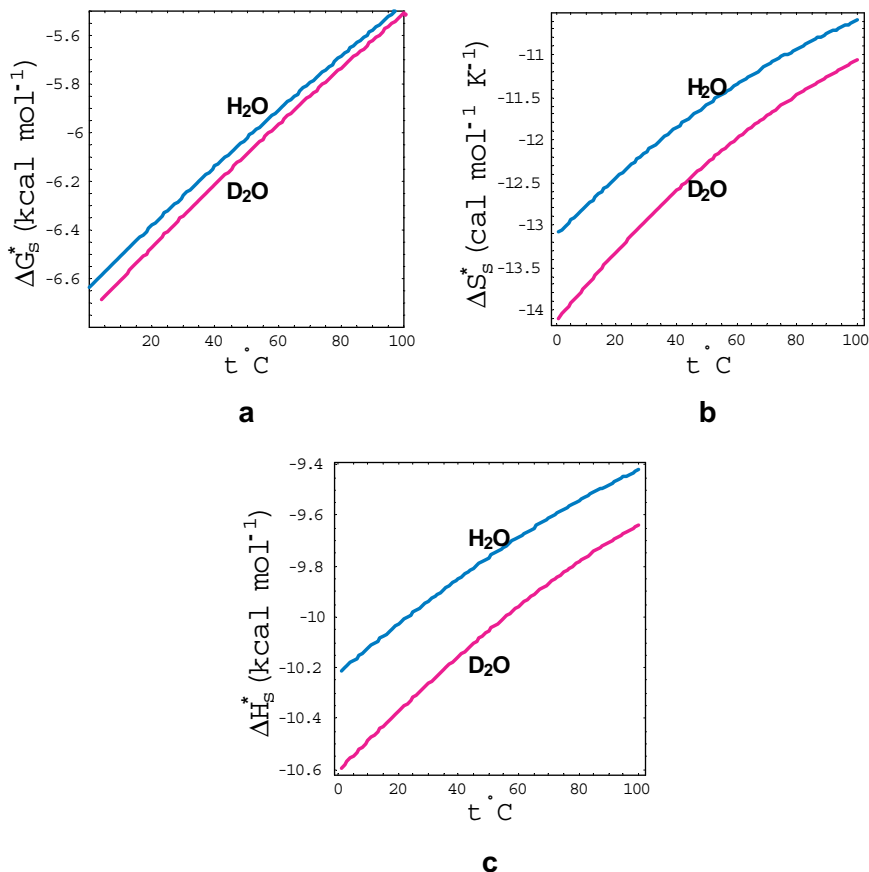


Fig. 1.45 (a) Solvation Gibbs energy, (b) entropy of solvation, and (c) enthalpy of solvation of water in water as a function of temperature.

cannot preclude the possibility of the existence of some other kind of life-form based on some other liquid.

As we have noted, the molar volume of ice is larger than that of liquid water. Everyone is familiar with the phenomenon of ice floating on top of water. If the molar volume of ice were *not* larger than that of water, ice formed on the surface of the ocean would sink to the bottom and then be insulated by the water covering it (water is a good thermal insulator). Over time, more

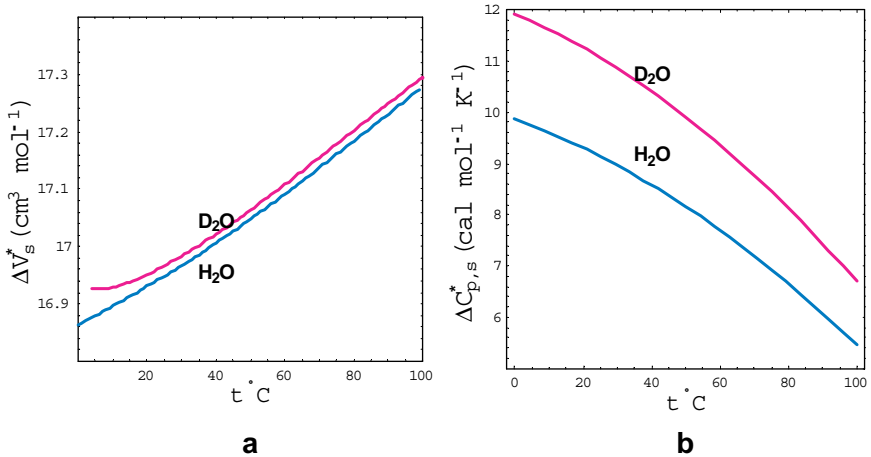


Fig. 1.46 (a) Solvation volumes, and (b) partial molar heat capacities of solvation of H₂O and D₂O.

and more layers of ice would accumulate on the bottom in a process that would gradually freeze nearly the entire ocean.

The fact that ice floats on top of the water helps to maintain the relatively high temperature of liquid water underneath — this in turn helps to maintain life in water in spite of lower temperatures above the surface. Clearly, when the temperature of the atmosphere increases, it is the ice on the surface that melts first — this too contributes to the maintenance of the water temperature underneath.

The fact that ice has a larger volume than liquid water can also be harmful to living organisms. When a living cell containing water freezes, the expanding ice can break the cell's membrane, possibly killing the cell. Some marine creatures that live in extremely cold environments possess a special “antifreeze” protein that lowers the freezing temperature and delays the process of ice formation.

The high value of the heat capacity of water is of primary importance in regulating the temperature of a living system. In

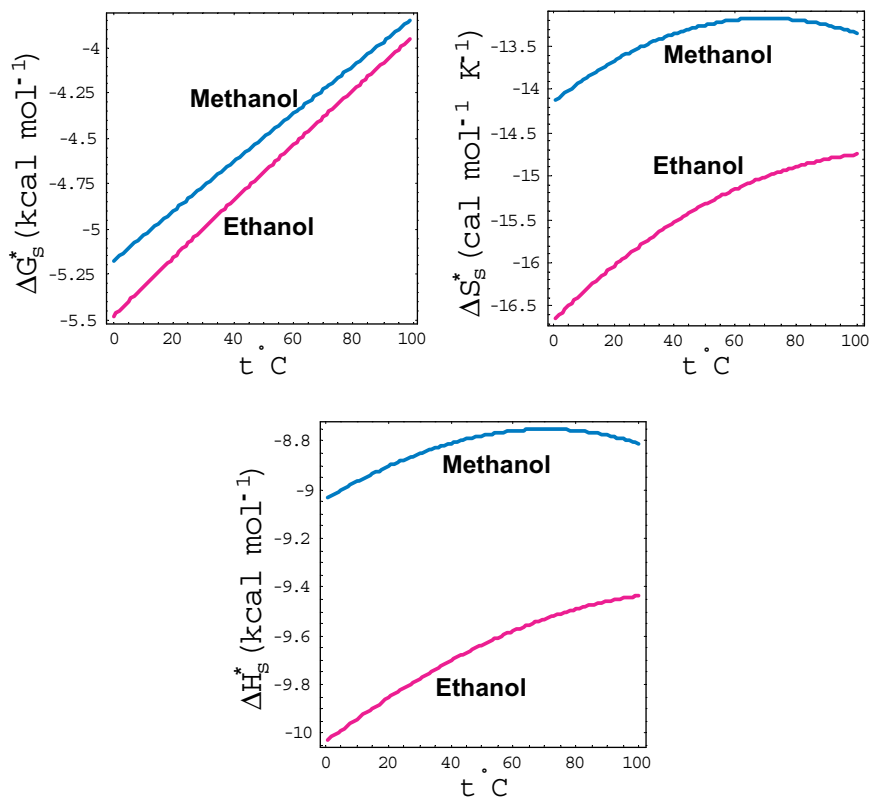


Fig. 1.47 Solvation quantities for methanol and ethanol.

each living cell, hundreds of chemical reactions take place. Some of these chemical reactions are exothermic, i.e. they release heat into the cell's surroundings. If this heat is not absorbed by some mechanism, the temperature will rise to a dangerous level. The large heat capacity of water means that for a given amount of heat absorbed by one unit volume of water, the temperature increase is smaller than it would be in a normal liquid. Thus, most of the heat released in chemical reactions is absorbed by the water — with a minimal increase in its temperature. This is also the reason why laboratories use water in a thermostat-bath when a constant temperature must be maintained. Because of its

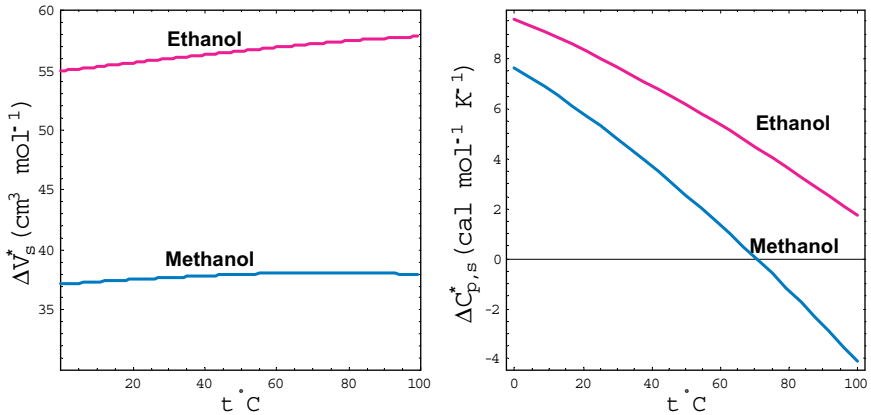


Fig. 1.48 (a) Solvation volumes, and (b) partial molar heat capacity of solvation of methanol and ethanol.

large heat capacity, the temperature does not change so rapidly as a result of heat flowing inside or outside the thermostat.

Another property of water that helps regulate body temperature is its large heat of vaporization. When the atmospheric temperature is high, both animals and plants evaporate some of their water content. This is the familiar phenomenon of sweating. Because the heat of vaporization of water is large, only a small quantity of water needs to be evaporated to maintain the temperature of the body. Note that the actual amount of sweat visible on the skin in hot weather or after exercising is not an indication of the amount of water that is evaporating. The evaporating sweat is released into the air as a gas and is not conspicuous. Sweat becomes visible only when liquid is released by the body more rapidly than the rate of evaporation. The rate of evaporation is affected by the relative humidity of the air. When the relative humidity is low, water evaporates quickly from the skin. When it is high, water evaporates slowly from the skin because the air has a lowered capacity to absorb additional water, and temperature regulation by sweating becomes

inefficient. This is the reason one feels more comfortable in the dry atmosphere of, say, Jerusalem than in the humid atmosphere of, say, Tel Aviv.

The large heat of vaporization helps to regulate not only the bodies of living organisms, but also the Earth's natural environment. Most of the radiant energy from the sun that reaches the Earth is absorbed by evaporating ocean water. The fact that the heat of evaporation of water is large, partially explains why this evaporation effectively prevents an increase in the Earth's temperature. If the seas were filled with some other liquid, e.g. alcohol, the Earth's temperature would sharply increase. Such an increase would probably kill all living creatures (assuming they had developed and were surviving in an "alcoholic" environment, which is doubtful).

We have mentioned the large amount of heat that is absorbed when ice melts, and the damaging effect of any water freezing within a living cell. If the temperature of pure water or any aqueous solution falls below the freezing point (which is normally lower for aqueous solutions than for pure water), ice begins to form and a large amount of heat is released. This release of heat decelerates the rate of any further ice formation, preventing or at least delaying the conversion of all the water in the body into ice.

In concluding this section, we mention two more properties of water that are important in biological systems. The first is a critical factor affecting the ability of plants to absorb water. This property is surface tension. Compared to "normal" liquids (e.g. alcohols, simple paraffins, and benzene), water has a very high surface tension. The surface tension of water at 20°C is about 72.75 (in ergs cm^{-2}), compared with acetone at 23.7, ethanol at 22.3, and n-hexane at 18.4, for the same temperature. This is significant because surface tension is the primary force that draws fluids up through capillaries. The higher the surface tension of a liquid, the higher the liquid can rise in capillaries.

This explains why water can rise in the interior of tall trees, even up to the highest leaves where it is needed in photosynthesis and temperature regulation.

The second property of water important for biological systems is the dielectric constant. The dielectric constant of water exceeds that of many liquids (for instance, hexane: 1.87; chloroform: 5.05; ethanol: 24; methanol: 33; water: 80; but hydrogen cyanide: 116). The dielectric constant of water is important for its capability of dissolving a great variety of molecules, from simple salts such as NaCl to very large molecules such as proteins. A more extensive discussion of the relevance of the properties of water to life may be found in Henderson (1913), Edsall and Wyman (1958), and Franks (2000).

The fact that the properties of water are “fine-tuned” to support life has been viewed as evidence of the existence of an Intelligent Designer. This is essentially the same argument as the so-called Anthropic Principle invoked by creationists in favor of the existence of an Intelligent Designer. If the Universe is so finely tuned to support life, the argument goes, there must be a “fine-tuner” who designed the Universe. In other words, an intelligent being has *designed* the Universe in such a way as to support life.

This type of argument is very appealing to those who believe that life as we know it on our planet is the only possible form of life. Still, one cannot exclude the possibility that other forms of life based on other liquids or even on different “fine-tuned” laws of physics could have evolved in some remote part of the Universe, or perhaps in other universes.

In Henderson’s (1913) book, “The Fitness of the Environment,” he discusses the reciprocity of Darwin’s fitness ideas and the fitness of water to life. He asks the question: “Water is indeed a wonderful substance which fills its place in nature most

satisfactorily, but would not another substance do as well? Is not ammonia, for example, a possible substitute?” Henderson concludes the chapter on water by the words: “In truth Darwinian features are a perfectly reciprocal relationship. In the world of modern science a fit organism inhabits a fit environment.”